AD

USAAVLABS TECHNICAL REPORT 68-34

A STUDY OF HIGH-MACH-NUMBER, HIGH-TEMPERATURE APPLICATION OF A SMALL, SINGLE-STAGE, AXIAL-FLOW GAS TURBINE

By

D. H. Cooke

June 1968

U. S. ARMY AVIATION MATERIEL LABORATORIES
FORT EUSTIS, VIRGINIA

CONTRACT DAAJ02-67-C-0011

ROCKETDYNE
A DIVISION OF NORTH AMERICAN ROCKWELL CORPORATION
CANOGA PARK, CALIFORNIA

93

Disclaimers

The findings in this report are not to be construed as an official Department of the Army position unless so designated by other authorized documents.

When Government drawings, specifications, or other data are used for any purpose other than in connection with a definitely related Government procurement operation, the United States Government thereby incurs no responsibility nor any obligation whatsoever; and the fact that the said drawings, specifications, or other data is not to be regarded by implication or otherwise as in any manner licensing the holder or any other person or corporation, or conveying any rights or permission, to manufacture, use, or sell any patented invention that may in any way be related thereto.

Disposition Instructions

Destroy this report when no longer needed. Do not return it to originator.

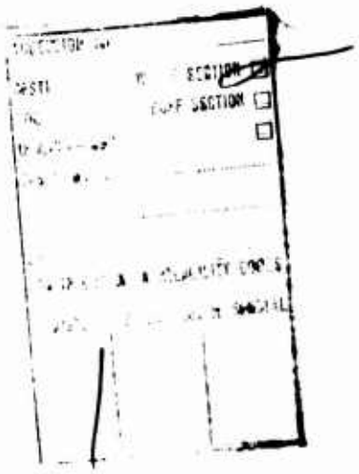

DEPARTMENT OF THE ARMY
U. S. ARMY AVIATION MATERIEL LABORATORIES
FORT EUSTIS, VIRGINIA 23604

Appropriate technical personnel of this Command have reviewed this report and concur with the conclusions contained herein.

The findings and recommendations outlined herein will be taken into consideration in the planning of future programs in the area of turbines and turbine engines.

Task 1M125901A01409
Contract DAAJ02-67-C-0011
USAAVIABS Technical Report 68-34
June 1968

A STUDY OF HIGH-MACH-NUMBER, HIGH-TEMPERATURE APPLICATION OF A SMALL, SINGLE-STAGE, AXIAL-FLOW GAS TURBINE

Rocketdyne Technical Report R-7261

By

D. H. Cooke

Prepared by

Rocketdyne
A Division of North American Rockwell Corporation
Canoga Park, California

for

U.S. ARMY AVIATION MATERIEL LABORATORIES
FORT EUSTIS, VIRGINIA

SUMMARY

The purpose of this study was to determine the merit and feasibility of using a single-stage axial turbine as a compressor drive (gasifier) turbine in a small, high-temperature, high-pressure-ratio, turboshaft/free-shaft engine. The size of the unit in terms of engine airflow was 5 lb/sec. Turbine inlet temperatures up to 2300°F, with cooling, compression ratios from 16:1 to 20:1, and shaft speeds from 50,000 to 70,000 rpm were investigated. Specifically, the objective of the study was first to determine by a generalized analysis the regions and relative levels of optimum performance within practical design limitations over the above ranges, and then to design and analyze in detail a turbine configuration selected as suitable to verify that the assumed operating conditions and limitations were realistic and practical. Of particular concern in the study were the occurrence and effects of supersonic velocities in the rotor blades, and the interrelation of stress and blade temperature in determining the optimum design.

The method used for the generalized analysis involved a computer design and optimization technique for axial gas turbines which features a similarity parameter approach and correlation of all significant losses in a turbine stage with geometry. The optimization was constrained to be within allowable stress and heat transfer limitations. The results of the generalized analysis showed that with cooling there is a broad design range with acceptable and competitive engine performance, within allowable stress limitations, over the full intervals of inlet temperature and pressure ratios investigated. Rotor inlet Mach numbers were found to be subsonic over the entire range, which eliminates the need for thin, sharp-leading-edge, supersonic blade designs, thus simplifying rotor blade cooling problems at high temperatures.

Upon completion of the generalized analysis, a configuration was selected for detailed design at 2300°F inlet temperature, 16:1 compressor pressure ratio and 63,000 rpm. The turbine had a pressure ratio of 3.88 and a $\Delta h/T$ of 0.073 Btu/lb°R. The rotor relative Mach numbers were 0.523 at inlet and 1.0 at exit. The detailed design showed that all aspects were within practical limitations. The final predicted turbine efficiency was 90.6 pct total-to-total and would result in a net engine specific power of 203.6 hp-sec/lb at a specific fuel consumption of 0.454 lb/hp-hr including cooling.

The major conclusions of the study are that single-stage, axial-flow gasifier turbines for the intended application are competitive in performance, have no Mach number penalties, are practical to build, and are within the reach of current advanced technology. They should result in significant improvements in weight, volume, simplicity, and cost over multistage components.

FOREWORD

This is the final report covering work done under Contract DAAJ02-67-C-0011 during the period beginning 6 February 1967 and ending 5 November 1967. The program was conducted under the direction of David B. Cale, representative of the Contracting Officer, U.S. Army Aviation Material Laboratories, Fort Eustis, Virginia. The program has been conducted within the Energy Conversion Systems Department, Small Engine Division, of Rocketdyne, under the cognizance of R. S. Siegler, Supervisor, and V. R. Degner, Department Manager. Acknowledgement is given to Dr. O. E. Balje, for consultation in developing the generalized analysis technique, and to the following personnel of the Rocketdyne Technical Staff who materially contributed: Dr. F. A. Shen, heat transfer analysis; R. L. Binsley, consulting turbine specialist; D. Staum, stress analysis; K. A. Wanner, design; V. L. Frank, computations.

CONTENTS

LIST OF ILLUSTRATIONS

LIST OF TABLES

INTRODUCTION

Recent trends in gas turbine engine development have been toward lighter, more compact power plants and have involved higher temperatures, pressure ratios, and rotational speeds. In turboshaft/free-shaft applications where the power turbine is on a separate shaft because of variable or reduced drive speed requirements, the gasifier, or the compressor-burner-turbine (gas-generator) combination, becomes a separate element. High speed is particularly important for this element because the compressor is more efficient and compact at high speeds, especially at high pressure ratios. The present level of gasifier speeds in engine development is such that a single-stage turbine theoretically has about the same level of efficiency as a multistaged unit, provided that limits in structural strength and supersonic losses are not too severe. A single-stage turbine is much preferable to multistaging from the standpoints of weight, volume, simplicity, and cost.

In a single-stage turbine, the pressure drop is expanded in a single step, whereas in a multistaged unit, it is broken up into several smaller expansions. The high nozzle velocities associated with the large expansion in a single-stage turbine require high blade speeds with associated high stresses to utilize the kinetic energy effectively. Also, in extreme cases, the expansion may produce supersonic velocities in the rotor blading, which, if not carefully designed, may produce excessive internal losses resulting from shock effects. These potential problems are compounded in applications involving high gas temperatures, because most available materials require cooling to preserve strength at elevated temperatures, and cooling is made much more difficult if sharp, thin, supersonic blade designs are required for good performance.

At the outset of this program, the difficulties and interrelation of high-pressure-ratio, stress, high-temperature, cooling, and high-Mach-number effects in a single-stage axial gasifier turbine were not clearly known for the 5-lb/sec engine under consideration. The purpose of this study was to investigate these difficulties and interrelations and to determine by optimization, followed by a careful, detailed analysis, the merit and feasibility of a single-stage axial gasifier turbine for the engine, over the specified ranges of engine operating conditions.

Because in a fixed weight-flow analysis, the gasifier turbine power level, and to a lesser extent the volumetric flow, depends upon the compressor performance, and because the selection of the best design point depends upon the resulting power turbine or net engine performance, it was considered most desirable to study the gasifier turbine in an engine context. It was decided that this could be effectively done by representing the compressor by approximate contours of efficiency as a function of design speed and pressure ratio. The basic data for these curves were received from the contracting agency. Both the gasifier and the power turbine were examined by using an existing turbine analytical and optimization technique which was converted to compressible flow and was refined considerably during this contract.

STATEMENT OF THE PROBLEM

The objective of this study was to design and determine the merit and feasibility of the single-stage axial turbine configuration which best lends itself to integration into a small, high-temperature, high-pressure-ratio, turboshaft/free-shaft engine. The size of the engine in terms of airflow is 5 lb/sec. The following ranges of engine operating conditions were specified:

Compressor Pressure Ratio	16:1 to 20:1
Turbine Inlet Temperature, °F	1700 to 2300

To accomplish this task, a theoretically developed design and optimization technique was to be used, as modified to include compressibility and Mach number effects and stress and heat transfer relations. This technique was to be applied in a generalized analysis to determine the tradeoffs among the independent variables (pressure ratio, temperature, rotational speed, and cooling level) and the dependent and geometric variables (rotor diameter, degree of reaction, blade and disc temperature, stress, and Mach number). These studies were to be used to select the most promising configuration for further detailed design and analysis to verify that the selected configuration was realistic and practical.

In the detailed design phase, the critical areas were to be carefully analyzed and integrated into a practical design. These areas were to include an aerodynamic blade design, a detailed heat transfer analysis of the blade, and a stress analysis with cooling. Integration and coordination of the design and analysis were to be accomplished through a detailed design layout, which would include an investigation of salient detailed mechanical and thermal effects.

Upon completion of the detailed design phase, a final performance calculation was to be made to incorporate modifications and compromises necessary to complete the detailed design task. An approximate part load performance evaluation down to the 40-percent power level was also to be included in the final performance calculation.

APPROACH TO THE GENERALIZED ANALYSIS

The approach to the generalized analysis involved development of a mathematical model of the engine and the establishment of pertinent ground rules regarding compressor performance, materials and structural design criteria to be used, cooling, and incidental losses.

MATHEMATICAL MODEL

The heart of the mathematical model was a recently developed generalized turbine design and optimization program (Reference 13), based on similarity parameters and including the major losses in a turbine stage. This program was based on concepts previously developed for turbines in Reference 1, namely, that five similarity groupings govern the efficiency of turbomachines. These groupings are:

1. The specific speed,

$$N_s = \frac{N\sqrt{V}}{H_{ad}^{3/4}} \tag{1}$$

where

N = rotative speed, rpm

V = exit volumetric flow, cu ft/sec

H_{ad} = isentropic heat, ft

2. The specific diameter,

$$D_s = \frac{D\, H_{ad}^{1/4}}{\sqrt{V}} \tag{2}$$

where

D = rotor tip diameter, ft

3. The Reynolds number, expressing the ratio of inertial forces to viscous forces, a parameter which becomes important for turbines operating at low back pressures with highly viscous media

4. The Mach number, expressing the ratio of a significant velocity in the velocity vector diagram to the corresponding sonic velocity, a parameter which is of significance in high-pressure-ratio turbines

5. The nature of the density change of the working fluid in the flow passages, which may be expressed for perfect gases by the ratio of specific heats, λ

The first two parameters reflect the velocity vector diagrams and are an index for the gas dynamic (i.e., pressure and velocity) conditions in the nozzle vanes and rotor blades. The gas dynamic conditions also reflect the turbine geometry and operating conditions. Because the relationships between the turbine geometry and losses are essential elements for determining the turbine efficiency, it follows that the specific speed and specific diameter are uniquely related to the most critical elements of the design.

Occasionally, other parameter groupings (e.g., head or velocity coefficient and flow factor) are used in the literature instead of specific speed and specific diameter. Such groupings have a similar significance but express the turbine dimensions of direct concern to the turbine designer (i.e., the rotor diameter and rotative speed) in an indirect form.

The work in References 13 and 1 developed relations and diagrams including the first three of the above groupings by limiting the analysis to incompressible flow. The work on this contract has extended the analysis to compressible flow, thereby including Mach number and the ratio of specific heats, and in addition has included stress limitations and heat transfer effects for a particular application.

The geometric parameters included in the optimizations of Reference 13 are as follows:

α_2 = nozzle exit design flow angle

$\frac{C_N}{D}$ = ratio of nozzle chord to annulus outside diameter

β_3 = rotor blade exit design flow angle

$\frac{C_R}{D}$ = ratio of rotor blade chord to rotor exit tip diameter

$\frac{h}{D}$ = ratio of rotor blade exit height to tip diameter

Other geometric parameters assumed as fixed for any particular optimization are:

$\frac{t_{bn}}{h}$ = ratio of nozzle vane trailing-edge thickness to exit height

$\frac{t_{br}}{h}$ = ratio of rotor blade trailing-edge thickness to exit height

$\frac{s}{h}$ = ratio of turbine tip clearance to exit blade height

$\frac{\Delta}{D}$ = ratio of average clearance between rotor disc and casing to rotor exit tip diameter (for disc friction losses)

α_1 = nozzle inlet design flow angle

Re* = characteristic Reynolds number

The solution and optimization technique for a given N_s and D_s involves finding the combination of the optimization parameters listed in the first group which maximizes the efficiency, subject to constraining relationships among the geometric variables (the continuity and energy equations). This is done by high-speed digital computer, using the direct-search, constrained optimization technique described in Reference 11.

The major losses included for full admission turbines in Reference 13 as functions of geometry and gas dynamic conditions are:

nozzle profile loss (including trailing edge loss)
nozzle end wall loss
rotor profile loss (including trailing edge loss)
rotor end wall loss
clearance loss
disc friction loss

Relations derived from boundary layer theory and cascade test data for these losses, and their sources, are given in Appendix D of Reference 13. The selection of these relations was based upon a careful survey of available data, in which adequate corroboration by test and consistency with theory were the main criteria. A comparison of the predictions used for profile and end-wall (secondary) losses with the range of other predictions may be seen in Figure 1.

The predicted profile losses in this study were based on maintaining optimum aerodynamic loading, the principle of which is shown in Figure 2. The aerodynamic loading may be expressed by the Zweifel coefficient (Reference 21), which is the ratio of the area of the actual pressure profile of the blade to the ideal area shown cross-hatched in Figure 2. This is expressed for compressible flow as

$$\psi_Z = \frac{t}{c} \frac{\sin^2 \beta_2 \, (1 + K_I)^2 \, \delta_u}{\sin \beta_s \left(1 + \frac{\gamma_2}{\gamma_1}\right)} \qquad (3)$$

where

ψ_Z = Zweifel coefficient

$K_I = \frac{C_{m1}}{C_{m2}}$ (see Figure 2)

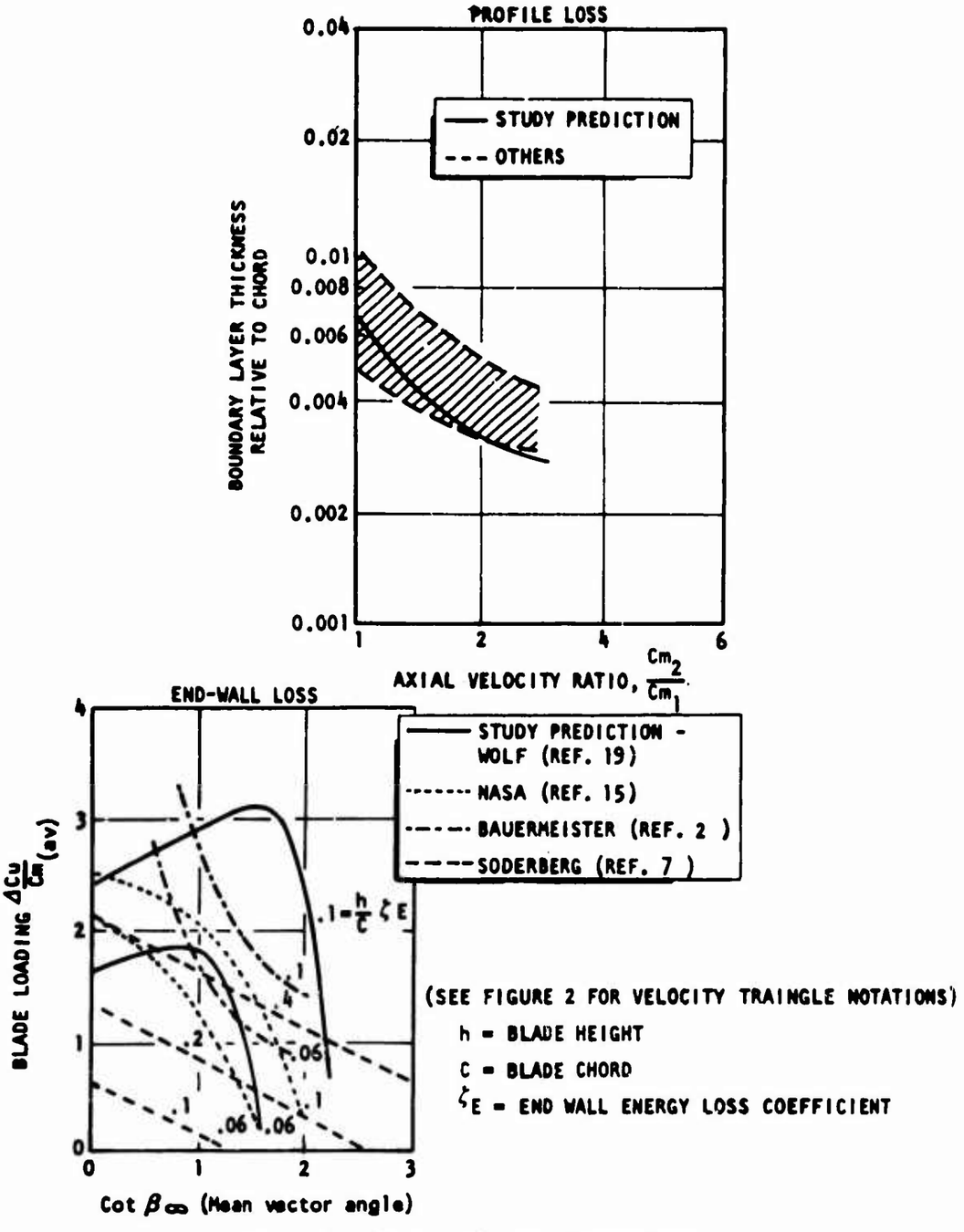

Figure 1. Basis of Loss Predictions

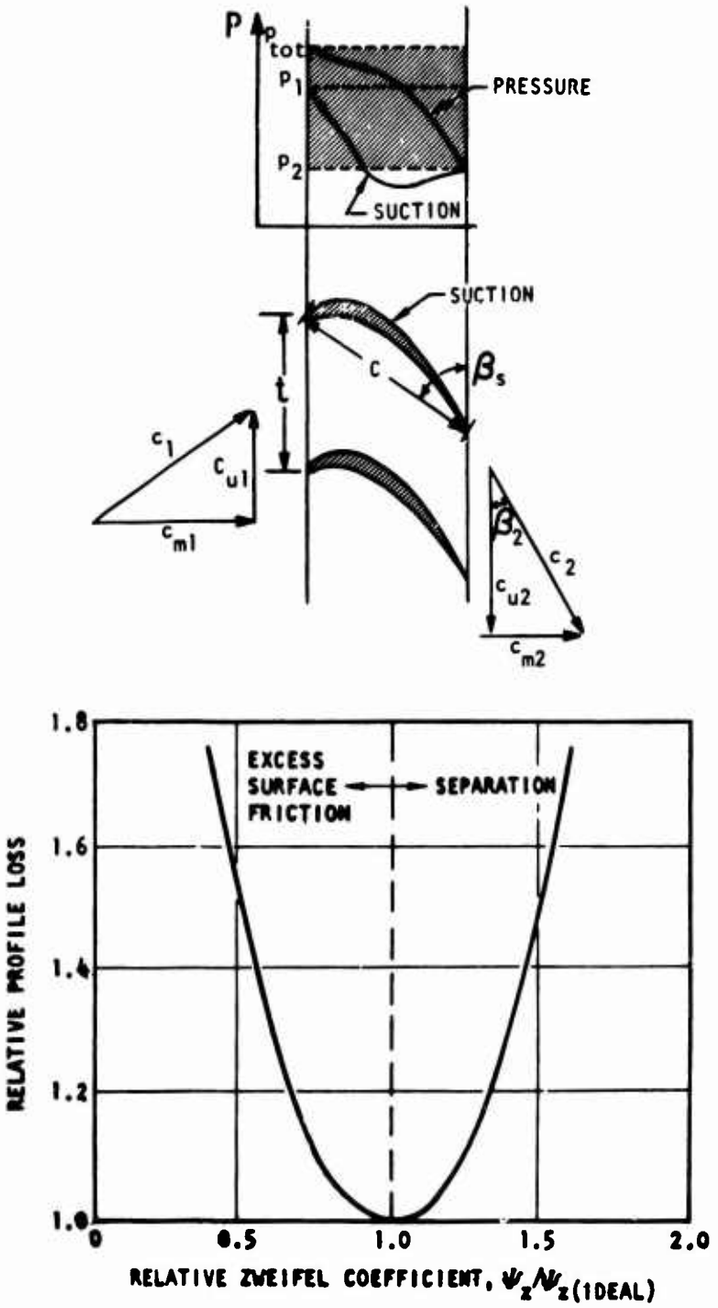

Figure 2. Optimum Aerodynamic Loading

β_s = Stagger angle

δ_u = $\frac{C_{u2} - C_{u1}}{C_{mav}}$ (see Figure 2)

γ = Density

It is shown in Reference 21 that the optimum aerodynamic loading for most cascade configurations occurs at a particular value of the ψ_Z such that the friction due to excess surface (too many blades) is minimized, and the loss due to separation (too few blades) has not begun to be predominant. The value of optimum ψ_Z used in this study was 0.9 for both the nozzle and rotor.

The end-wall loss is particularly subject to a wide range of experimental data as can be seen in Figure 1. The data of Wolf (Reference 19) are believed to be better substantiated by test than other sources and involve a recognition of boundary-layer history dependence not included elsewhere. The failure to recognize this effect is believed to be a major source of the wide variation of data. The term "history dependence" refers to the initial end-wall boundary layer which may exist at entrance to the nozzle vanes. The mechanism of end-wall loss, which is caused by the storing of energy in vortices generated by the turning of a nonuniform velocity distribution in the vanes, may be seen in Figure 3. If the initial end-wall boundary layer is as little as 3 pct of the blade height, as can be the case with a long entry section, the result will be an increase by a factor of three in end-wall loss coefficient, which means a loss of about two points in turbine efficiency for low-aspect-ratio designs such as those in this study. The end-wall losses used in this study are based on zero initial boundary layer thickness, which can be closely approached in a well designed engine.

The efficiencies predicted for the gasifier turbine of this study may appear to be quite high in comparison with data on some similar turbines in the recent literature. It should be emphasized that these predictions are based on complete, simultaneous, computer optimization of the several geometric parameters, as opposed to a limited optimization of only one or two parameters with other variables held fixed. The improvement in performance over limited optimization techniques may amount to as much as three points in efficiency. It should also be pointed out that the efficiencies represented here are for a "finely tuned" design, after corrections for variations in flow angles caused by rotational effects. Such corrections in "first build" engines typically result in a one- or two-point improvement in turbine efficiency for the production engine.

The similarity concept makes it possible to graphically represent the turbine efficiency as a function of specific speed and specific diameter in generalized charts which hold true regardless of physical size or power level. Such a chart showing total-to-total efficiency and optimum

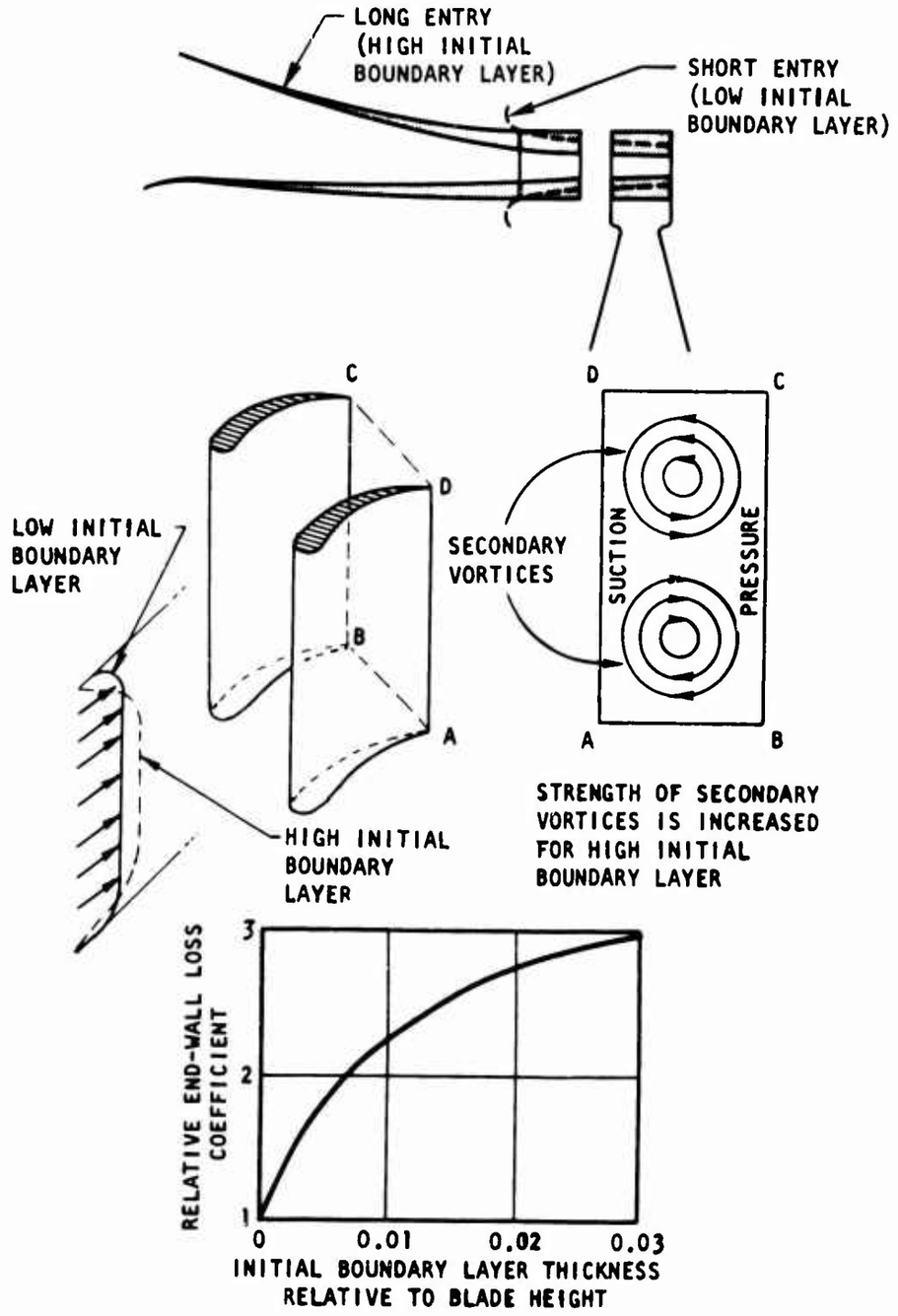

Figure 3. Initial Boundary Layer Effect

height-to-diameter ratio contours is shown in Figure 4, which includes a comparison of several test data points from the literature with the prediction method used in this study. In correlating the data, corrections have been made for non-optimum height-to-diameter ratio and Reynolds number, according to curves given in Reference 13.

A more complete chart showing total-to-static efficiency contours is shown in Figure 5. Certain of the variables associated with the optimum geometry and gas dynamic conditions are shown on this diagram.

In addition to h/D, these are:

$(C_3/C_o)^2$ = ratio of exhaust energy to isentropic available energy

ρ = reaction, defined isentropically as the ratio of static-to-static expansion energy in the rotor to the total-to-static expansion energy across the stage

Even though the diagrams of Figures 4 and 5 are for incompressible flow, the efficiency islands and the other parameters are not widely different from those for compressible flow in cases where the losses caused by high-Mach-number effects are small.

As a first task on this program, a preliminary engine configuration analysis was performed using the incompressible results. This was done as a prelude to technique and code modifications to indicate the scope of modifications necessary. The range of gasifier turbine designs is shown by the heavy lines overlaid on the chart (Figure 5). The long diagonal lines represent lines of constant velocity ratio (blade to isentropic) for the limits of operating conditions specified, with the gasifier turbine properly matched in the engine. The dashed and dotted lines indicate the design ranges with regard to inlet temperature and speed. The close proximity of single-stage gasifier turbines to the region of peak efficiency confirms that multistaging would not appreciably improve theoretical performance.

Among the indications from this preliminary study were that rotor sonic conditions would be in the high subsonic to transonic regime with subsonic inlet, and that stress limits on diameter and blade height to stay safely within material strength, particularly for the high inlet temperatures, would be severe.

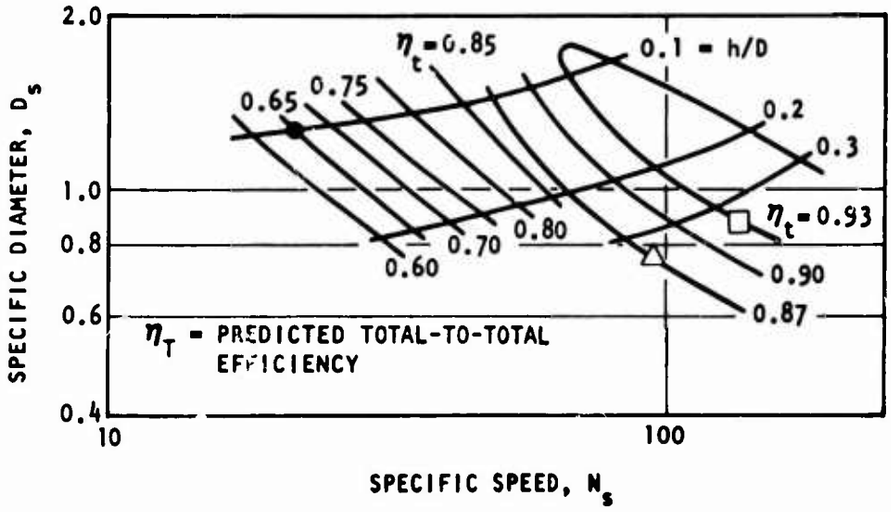

SYMBOL	REF.	h/D	η_{TEST}	η^*	η^{**}
●	11	0.064	0.60	0.62	0.66
△	18	0.15	0.86	0.89	0.89
□	12	0.2	0.89	0.92	0.92

NOTE:

η_{TEST} = TESTED TOTAL-TO-TOTAL EFFICIENCY

η^* = η_{TEST} CORRECTED FOR OPTIMIZATION OF H/D (REF. 13)

η^{**} = η^* CORRECTED FOR REYNOLDS NUMBER (REF. 13)

Figure 4. Comparison With Test Data

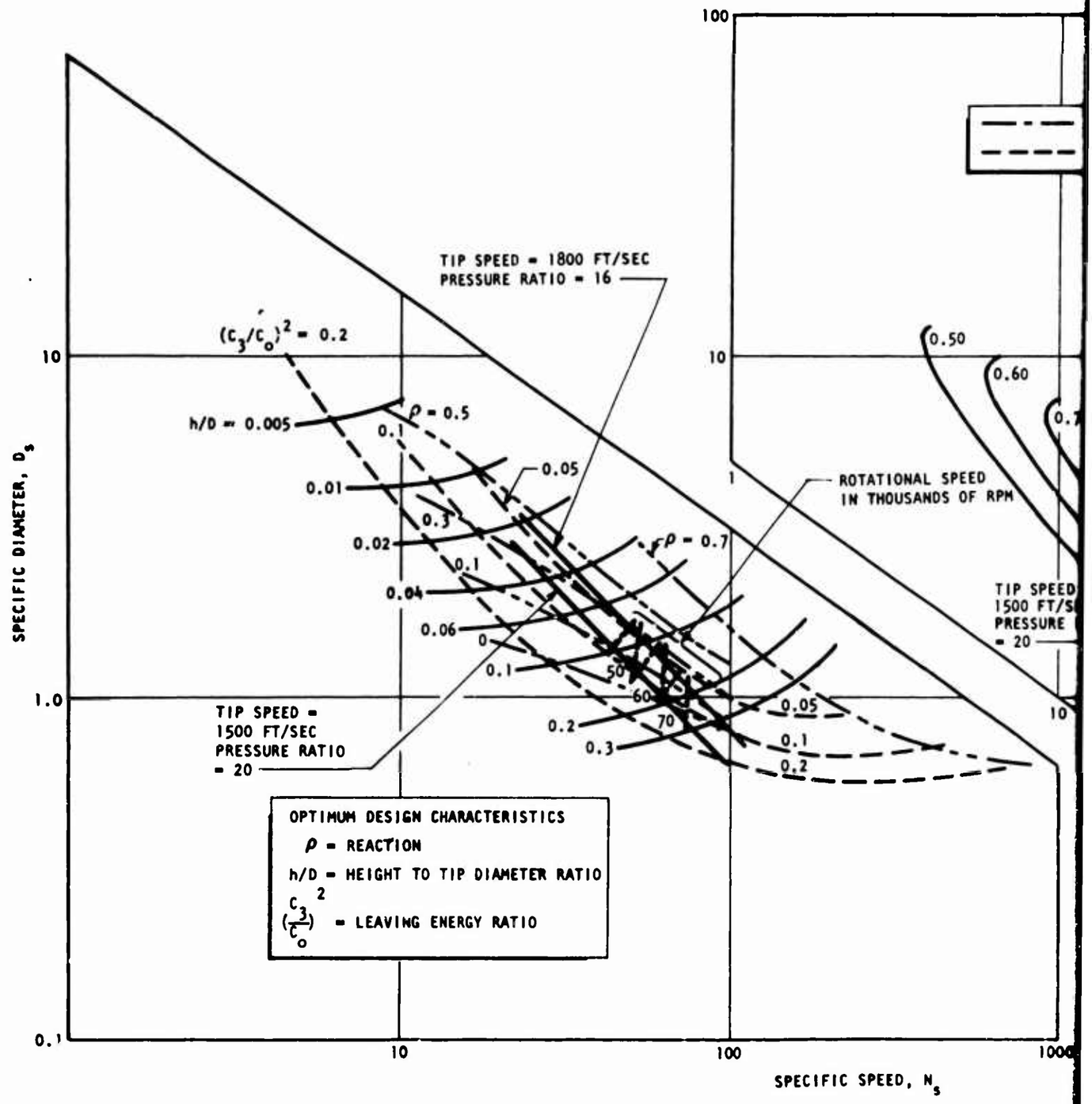

Figure 5. Turbine Design Chart (Incompressible) Showing Approximate Gasifier Turbine Design Regions

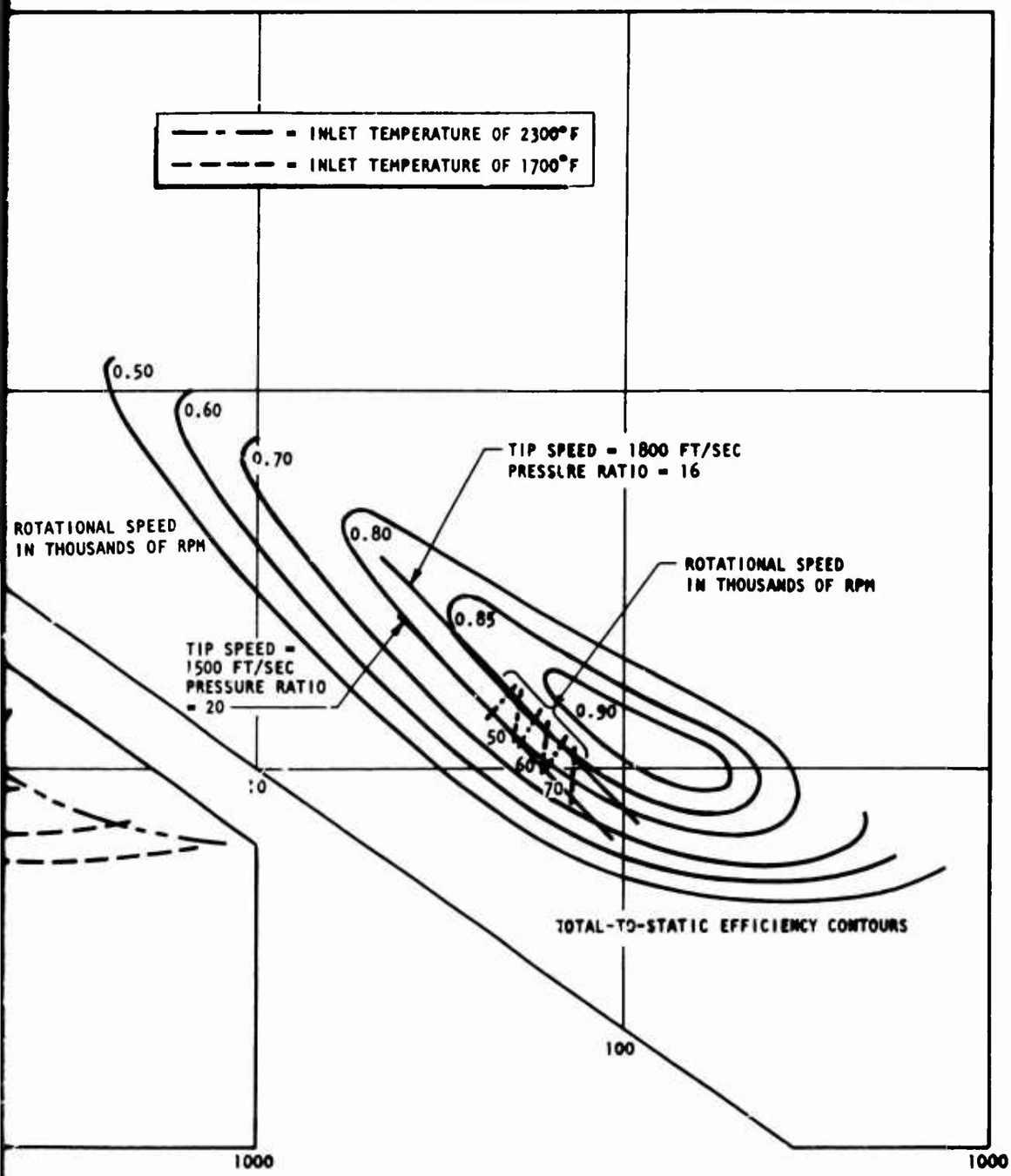
— - — = INLET TEMPERATURE OF 2300°F
— — — = INLET TEMPERATURE OF 1700°F
0.50
0.60
0.70
0.80
0.85
0.90
TIP SPEED = 1800 FT/SEC
PRESSURE RATIO = 16
ROTATIONAL SPEED
IN THOUSANDS OF RPM
TIP SPEED =
1500 FT/SEC
PRESSURE RATIO
= 20
ROTATIONAL SPEED
IN THOUSANDS OF RPM
50
60
70
:0
TOTAL-TO-STATIC EFFICIENCY CONTOURS
100
1000
1000
IC SPEED, N_s

B

Compressibility and Three-Dimensional Revisions

The addition of compressibility and Mach number effects to the basic program consisted in rederivation of equations and relations for losses in Reference 13, and the additions to the losses so as to cover the range of investigation. Also included were three-dimensional relations to provide an approximate integrated average of losses at hub, mean and tip, because it was apparent that velocity triangles would change considerably from hub to tip due to the turbine vortex effect.

The addition of compressibility added the following parameters to the direct search optimization:

$\frac{A_3}{A_2}$ = annulus area ratio between rotor exit and nozzle exit

$\frac{A_2}{A_1}$ = annulus area ratio between nozzle exit and nozzle inlet

These were constrained in the optimization to limit the meridional angle between the nozzle and rotor blade at base and tip to 10 degrees or less so as to prevent flow separation.

Additions to the fixed parameters were:

λ = average ratio of specific heat during the expansion

M_o = characteristic Mach number

$$= \frac{C_o}{\sqrt{\lambda g R T_3}}$$

where

C_o = isentropic velocity (stage)

T_3 = static temperature at rotor blade exit

R = gas constant

Inclusion of Stress Constraints

The inclusion of stress constraints was accomplished through the dimensionless stress factor

$$S = \frac{\sigma g}{U_t^2 \rho_m}$$

where

σ = stress, which may be limited to the allowable stress which is a function of material, temperature, and mission life

g = gravitational constant

U_t = turbine tip speed

ρ_m = material density

There are two separate and distinct stress factors, one for the disc and one for the blade root. Both of these may be expressed as functions of h/D, as shown in Figure 6.

The disc stress factor is also a function of the disc taper ratio, as shown, and the root stress factor is a function of blade area taper ratio (cross-sectional area at tip/cross-sectional area at base), as shown in the figure. Both of these are more or less fixed limiting parameters which may be readily assigned for a given general turbine design region. The selection of these parameters will be clarified under the discussion of ground rules later in this section.

It may be seen from Figure 6 that the range of h/D may be roughly divided into two regimes, depending on which stress factor is predominant. For low h/D, the disc stress factor is predominant, which means that the disc stress will be higher than the blade-root stress for a given tip speed, assuming that the disc taper is limited by design considerations to a fairly low value.

The designs considered in the study were generally in the low h/D region. Therefore, the procedure followed in accomplishing the stress constraints was to specify a limiting tip speed based on the disc material strength with appropriate safety factors, assuming an average disc stress factor chosen to provide a moderate disc taper. An upper limit on the blade-root stress factor, and hence h/D, was then provided by specifying the blade allowable stress as a function of temperature.

Because there was a possibility, with the tip speed fixed and the blades stress limited, that the design might be forced into a nonoptimum region, it was necessary periodically to test the validity of the optimization by trying a lower tip speed. A lower tip speed would allow a larger blade-root stress factor and h/D. In all cases, it was found that the tip speed was predominant in influencing the efficiency; that is, lower tip speeds resulted in lower efficiency even in cases of severely limited h/D.

A survey of tip speeds above and below the limiting value set by the disc stress was made to show the tip speed effect on performance. The results are shown in Figure 17 which will be presented in a later section.

As illustrated in the lower portion of Figure 6, for a given rotational speed, a blade stress limit results in an effective limit on annulus area,

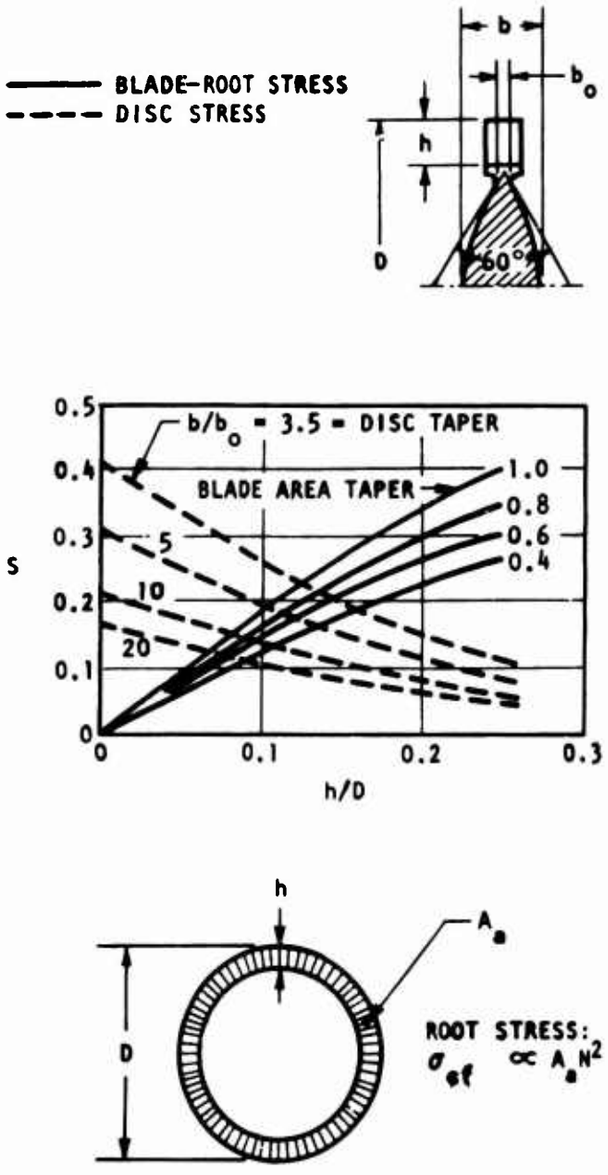

Figure 6. Stress Relations

because blade centrifugal stress, σ_{cf}, is proportional to the annulus area, A_a, times the square of the rotational speed, N^2. This, in extremely stress-limited cases, results in choking of the annulus area above a certain speed, because of sonic conditions; i.e., reaching the minimum area required for passing the specified mass flow under the upstream pressure and temperature conditions.

Inclusion of Heat Transfer Relations

In view of the fact that the higher specified inlet temperatures were surely to require cooling with any known materials, but the particular technique of cooling to be used was not clear, it was considered most expeditious in the generalized analysis to assume a simplified, idealized method of cooling. This would provide a means of assessing relative levels of cooling required for the different designs, even though the effectiveness of the idealized technique, and thus the absolute cooling level, might be different from any real technique.

The method selected was that of removing heat at the base of the blade in an infinitesimally thin cylinder concentric with the turbine axis. The blades were assumed to act as cylindrical fins projecting radially into the hot-gas stream.

At the base of the blade, the heat to be removed externally was corrected for heat entering the disc by conduction to a hub region at a specified fixed temperature. To provide this quantity, a disc design program was included which provided an optimum disc profile, with the thickness at each radial station determined so as to be just within the allowable stress at the local temperature. Both thermal and centrifugal stresses were included in the calculation.

Adaptation for Generalized Engine Study

The compressible flow turbine optimization code was integrated into an engine design code by providing compressor matching and power turbine subroutines.

The procedure used for compressor matching is illustrated by the cycle T-S diagram in Figure 7. Correct matching of turbine and compressor requires that the heads H_c and H_g be equal, with the rotational speed the same. The compressor head H_c was known from the assumed curves of compressor performance provided by the contracting agency. Because H_g depends on the turbine efficiency, which is not known in advance, an iteration was required. This was effectively closed using the high-speed digital computer technique. Upon closure, the residual head between the resulting gasifier turbine exhaust state point and the ambient pressure was used to calculate the optimum-power turbine performance under the available conditions. This is H_{adp} in the figure.

For simplicity, the power turbine was calculated as a single-stage turbine even though it was realized that the resulting drive speeds might be excessive for the application. The performance of single- and multi-staged

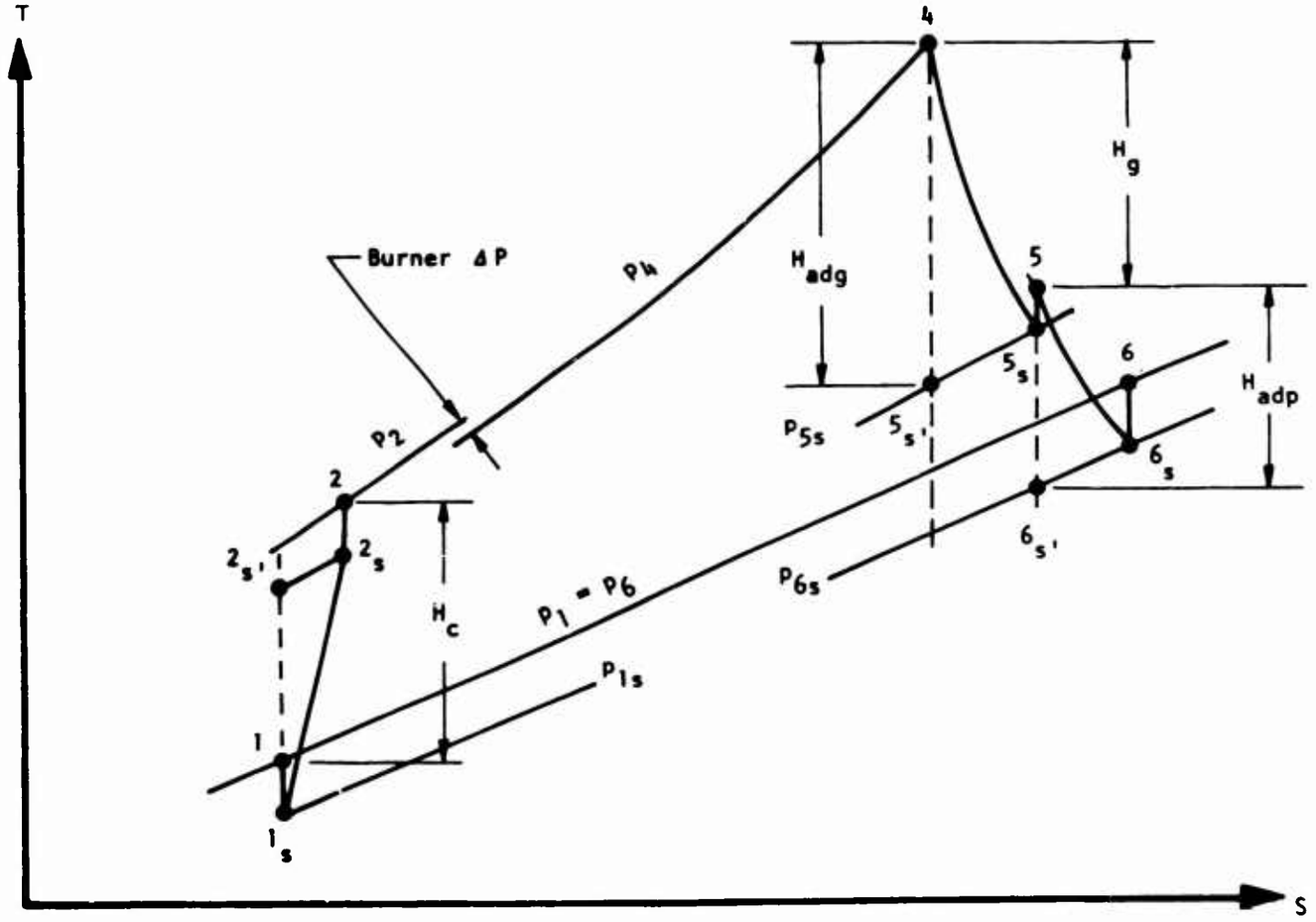

Figure 7. Schematic Cycle Diagram

units in the power turbine specific-speed range is substantially equivalent, however, so that the resulting engine performance is representative of multistaged units at lower speeds. Net power turbine efficiencies in the region of the study ranged between 85 and 90 percent.

A schematic diagram of the completed digital computer program is presented as Figure 8.

GROUND RULES FOR THE ANALYSIS

Compressor Performance

The compressor performance assumed for the generalized study was intended to be representative of an advanced, high-speed, transonic-axial, and centrifugal stage combination. The range of assumed performance as a function of pressure ratio and speed is shown in Figure 9. The curves were established using an existing technology curve, also shown in the figure, which was provided by the contracting agency. It was assumed that the advanced compressor would be capable of a net "target" efficiency of 83 pct at a compressor pressure ratio of 16:1. Comparisons were made of cycle and gasifier turbine performance for the advanced and existing technology compressors in the study, but the main survey of performance was made using the advanced compressor data.

Structural Design Criteria and Materials

As described in the previous discussion of stress constraints, the two general stress limits involved were the disc stress and blade-root stress. Because all of the designs investigated fell generally in the "low-blade-height" regime, the blade tip speed was primarily limited by the disc stress. The design criterion assumed for the disc, to establish maximum allowable tip speeds for the generalized analysis, was that of providing a burst speed of 135 pct of maximum operating speed, based on a burst stress of 85 pct of "typical" ultimate strength. This was combined with a reasonable limit of the disc taper angle (Figure 6) to about 60 degrees, which was considered prudent design practice. This is ensured by limiting the dimensionless stress factor, S, for the disc to 0.2.

Using the foregoing basis, we find that the maximum allowable tip speeds fall into two categories, depending on whether the disc is forged or cast. This is because of the fact that cast materials generally have lower ultimate strengths in the temperature range of the disc than forged materials.

Assuming INCO 713C as a typical cast material and an ultimate strength of 125,000 psi at 1000°F, we find that the resulting maximum tip speed is 1600 ft/sec. With INCO 718 as a typical forged material, the ultimate strength is 185,000 psi and the maximum tip speed is 1900 ft/sec. This established 1600 to 1900 ft/sec as a range of limiting tip speeds for the generalized analysis.

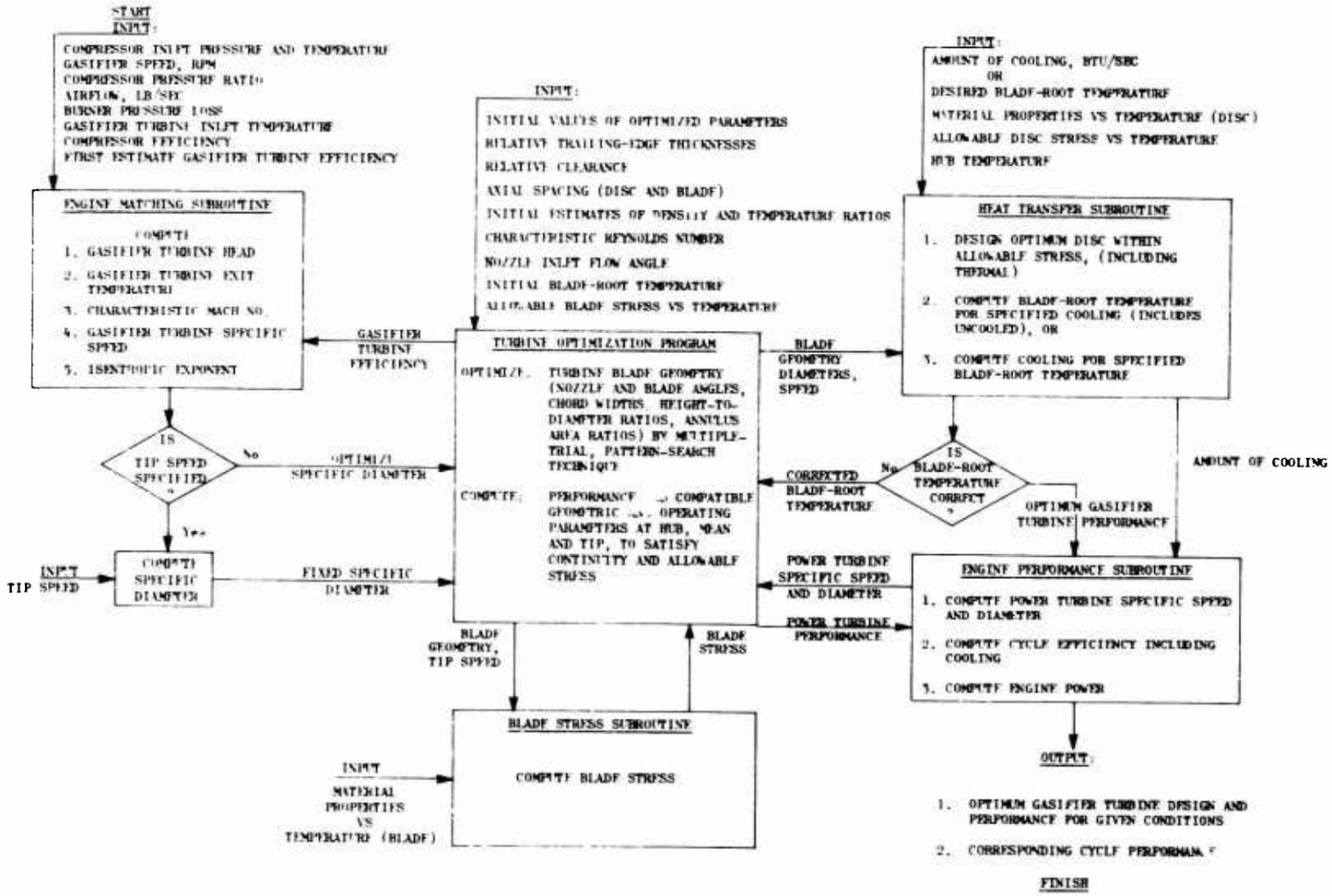

Figure 8. Schematic Diagram of Gas Turbine Engine Design Computer Program

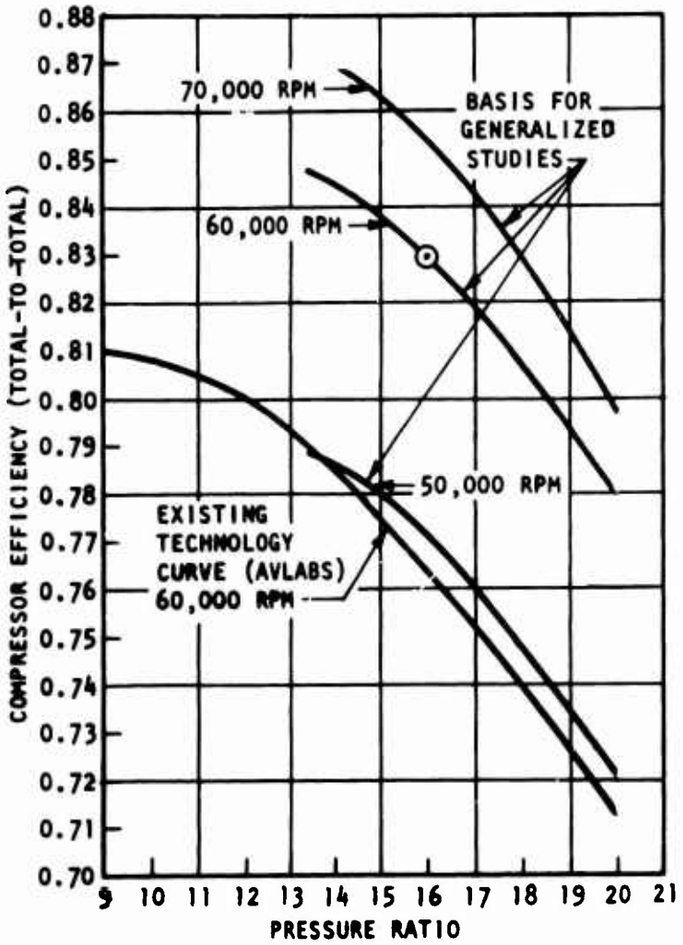

Figure 9. Assumed Compressor Performance

It was assumed that the blade materials would be cast because of the higher rupture strengths for cast materials in general at temperatures above 1200°F. Also, investment casting techniques seemed most promising for the expected cooled blade configurations. INCO 713C was selected as a typical blade material. (This was later changed to IN-100 in the detailed analysis because of slightly better properties.)

The structural design criteria for the blades was based on the typical 100-hour rupture strength, as shown for INCO 713C in Figure 10. This rupture strength duration was selected with approval of the contracting agency, on the basis that the mission life of the engine at full power and temperature would be a fraction of the ultimate life of the engine, rated at a lower power and temperature.

The safety margins assumed are also illustrated in Figure 10. A basic stress safety factor of 1.5, times an overspeed allowance factor of 1.21 (10-percent overspeed), times a factor of 1.15 to allow for minimum guaranteed strength, resulted in the allowable mean stress curve shown in the figure. A further allowance for bending and vibratory stresses of 10,000 psi was subtracted, giving the allowable direct centrifugal stress curve shown.

For the generalized analysis, the blades were assumed not to be tapered radially. It was later found that an area taper could be effectively designed into the cooled blade, thus permitting operation at about 150°F higher blade temperatures than shown in the generalized analysis.

Cooling Assumptions

The idealized cooling technique assumed for the generalized analysis was described in a previous section. The blade-fin assumption with lumped heat removal at the base resulted in heat removal rates of about 1 pct of the net engine power to achieve blade-root temperatures of 1200° to 1300°F at 2300°F inlet temperature. The 1-pct idealized heat load was therefore adopted as standard at 2300°F to evaluate the effects of various design changes at the same cooling level. The effect on performance of varying the blade-root temperature was also investigated.

To include the effect of the disc heat transfer, a wheel hub temperature of 750°F was used.

Incidental Losses

A burner pressure loss of 2 pct and a burner efficiency of 98 pct were assumed in determining pressure and performance levels.

The efficiency of the exhaust duct diffuser from the gasifier turbine to the power turbine was assumed as 50 pct for most of the generalized analysis. This was considered to be a reasonable level for absolute exit Mach numbers of 0.4 to 0.6. However, for the highly stress limited cases where the absolute exit Mach numbers approached unity, efficiencies that

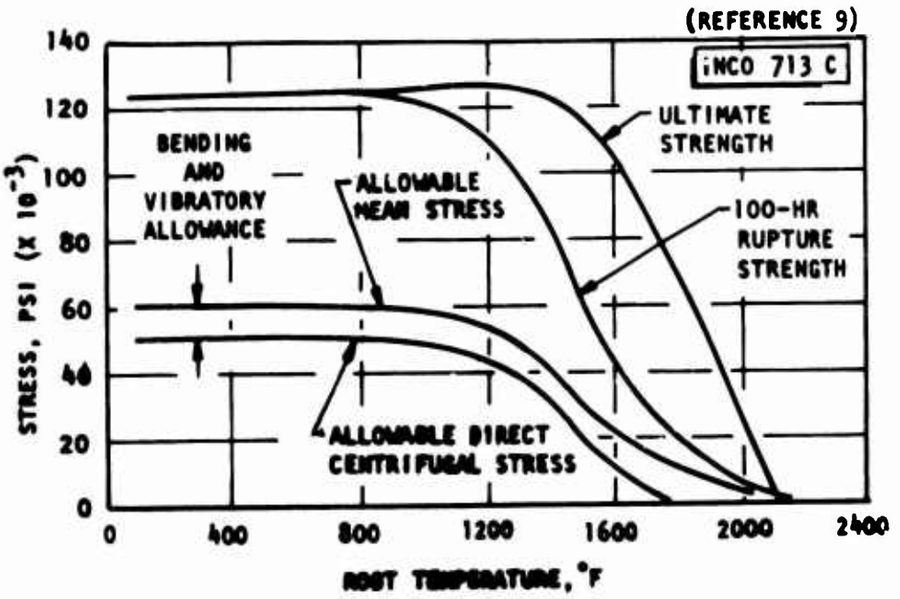

Figure 10. Blade Material and Structural Design Criteria

decreased progressively with increasing Mach number were used, down to a level of 20 pct, according to an estimate based on the larger diffusion angles with the shorter blades.

RESULTS OF THE GENERALIZED ANALYSIS

ENGINE PERFORMANCE AND OPTIMUM CONDITIONS

General Survey at 2300°F and 1700°F

The engine performance contours for 2300°F inlet temperature at a nominal heat load of 1 pct of the net engine power, based on the advanced compressor design, are shown in Figure 11. Blade-root temperatures vary between 1200° and 1300°F over the ranges, being in the vicinity of 1300°F for 1600-ft/sec tip speed and 1200°F for 1900 ft/sec. The 1-pct heat load refers to the quantity of heat energy entering the blade from the hot gas and leaving at the root to the external cooling medium and to the hub through the disc, based on the assumed idealized cooling technique. Nozzle cooling is not included in these generalized studies.

Gasifier turbines and engines for the lower tip speed designs have poorer performance than the higher tip speed designs for two reasons. The first is the obvious reduction in isentropic velocity ratio (U/C_o) and poorer utilization of kinetic energy. The second reason is less obvious; the blade heights for the lower tip speed are larger and tend to absorb more heat from the hot gas. Therefore, the designs for 1600 ft/sec have slightly higher blade temperatures and consequently lower allowable stresses. The blade annuli for the 1600-ft/sec designs are thus more restricted by stress limits, causing poorer performance because of higher velocities and increased losses. The peak total-to-static efficiency at 1900 ft/sec is 85 pct; at 1600 ft/sec it is 79 pct.

The specific horsepower and thermal efficiency values in Figure 11 and those following in this section have not been corrected for the engine power penalty because of cooling. This is equivalent to assuming cooling from an external source with no change in engine design or performance resulting from the cooling mechanism. In the detailed design phase, the modifications to effect cooling by a practical self-contained technique are included.

The thermal efficiency values may be converted directly to specific fuel consumption using the formula

$$SFC = \frac{0.13826}{\eta}$$

where

SFC = specific fuel consumption, $\frac{lb}{hp\text{-}hr}$

η = thermal efficiency

This assumes a fuel heating value of 18,400 Btu/lb.

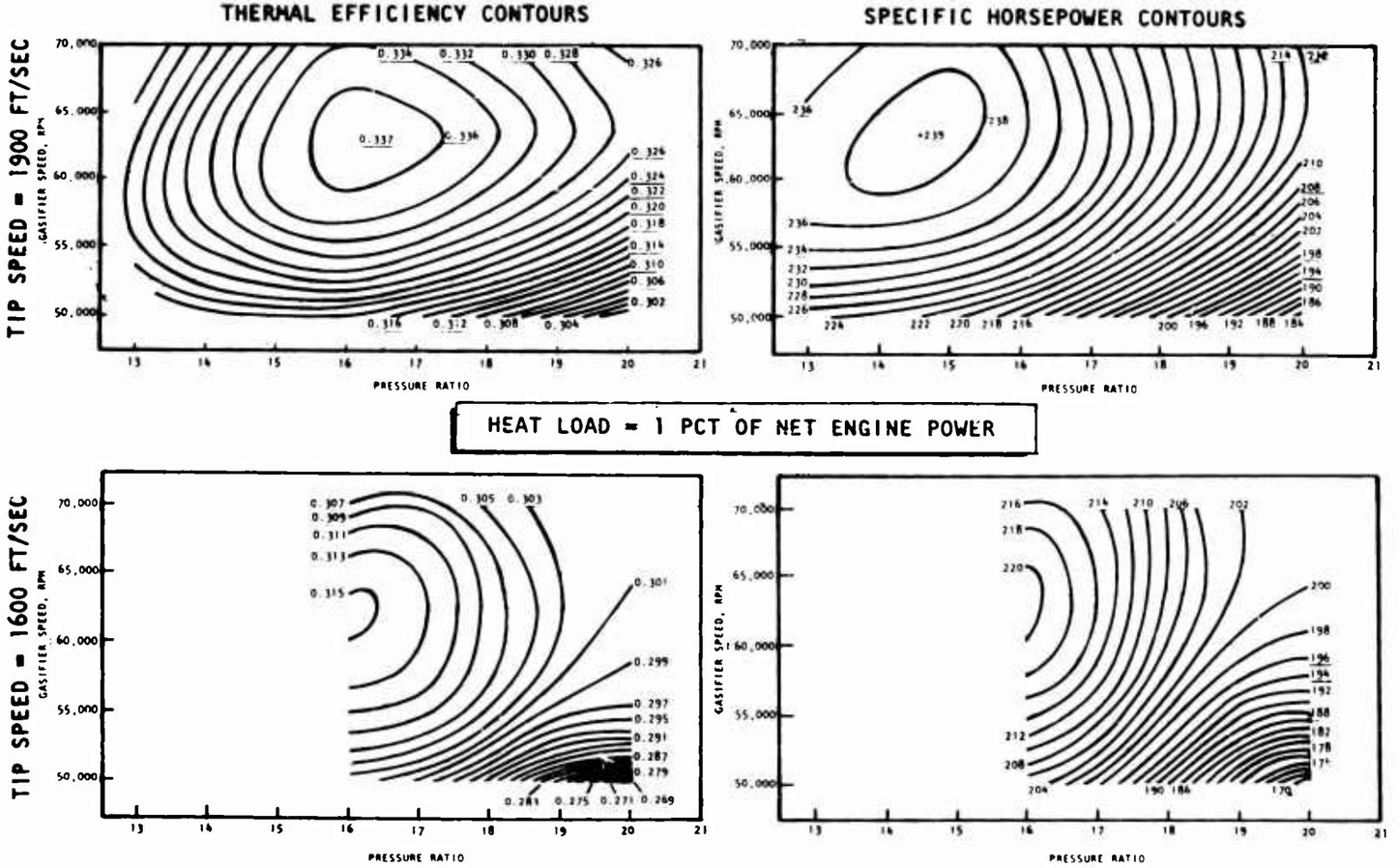

Figure 11. Engine Performance, 2300°F Inlet

The performance of an uncooled engine at 1700°F inlet temperature is shown in Figure 12. The striking effect of blade-root temperature and allowable stress may be seen in the distortion of the contours. In the high-speed, low-pressure-ratio regions, the blade recovery temperature was highest, as shown. This caused higher blade temperatures and lower allowable stresses, restricting the designs to smaller annuli and h/D, which caused impaired performance. This effect did not appear in the survey of cooled designs in Figure 11, because in order to simplify the calculation, strict control of the heat load at exactly 1 pct was not imposed. The heat load was allowed to vary ±10 pct with a constant blade temperature. Strict control at zero external cooling was imposed in Figure 12.

The 1700°F engine performance in Figure 12 probably had attained peak thermal efficiency before blade temperature-stress limitations became predominant, judging from the shape of the islands. However, a slightly lower inlet temperature might result in an improvement in specific power, because it appears that the specific power should peak at about 13:1 pressure ratio, at the same speed as the efficiency peak in a region of impaired performance. It is worth mentioning that selection of a lower tip speed would not improve the distortion, because the blade temperatures are increased at lower tip speeds.

The gasifier turbine efficiency contours shown in Figure 12 and elsewhere in the section are total-to-total; i.e., the exhaust energy is not charged to the gasifier turbine. This is merely an academic distinction, because the net engine performance reflects the loss of exhaust energy in the ducting.

Inlet Temperature Effects

The effect of inlet temperature on engine performance may be seen in Figure 13. Again, these curves do not include the engine power penalty resulting from cooling, but they serve to illustrate that the major gain from high inlet temperature is in specific power rather than specific fuel consumption. The increase in potential specific power by increasing the temperature from 1700° to 2300°F is about 86 pct, or nearly double, while the improvement in thermal efficiency is only about 10 pct. The small gain in thermal efficiency is almost certain to be lost in the cooling power penalty associated with accommodation of the heat load.

The heat load in Figure 13 is assumed to vary linearly between 1700° and 2300°F. It is not zero at the "uncooled" 1700°F because the heat flow into the disc is included.

Cooling and Blade Temperature Effects

The effect of a self-contained cooling system on engine performance is shown in Figure 14 for the two limiting tip speeds, 1600 and 1900 ft/sec. Provided the penalty to net engine power can be held to 8 pct, the available specific power is still substantially in excess of that of an uncooled engine, while the thermal efficiency (specific fuel consumption) is not appreciably different.

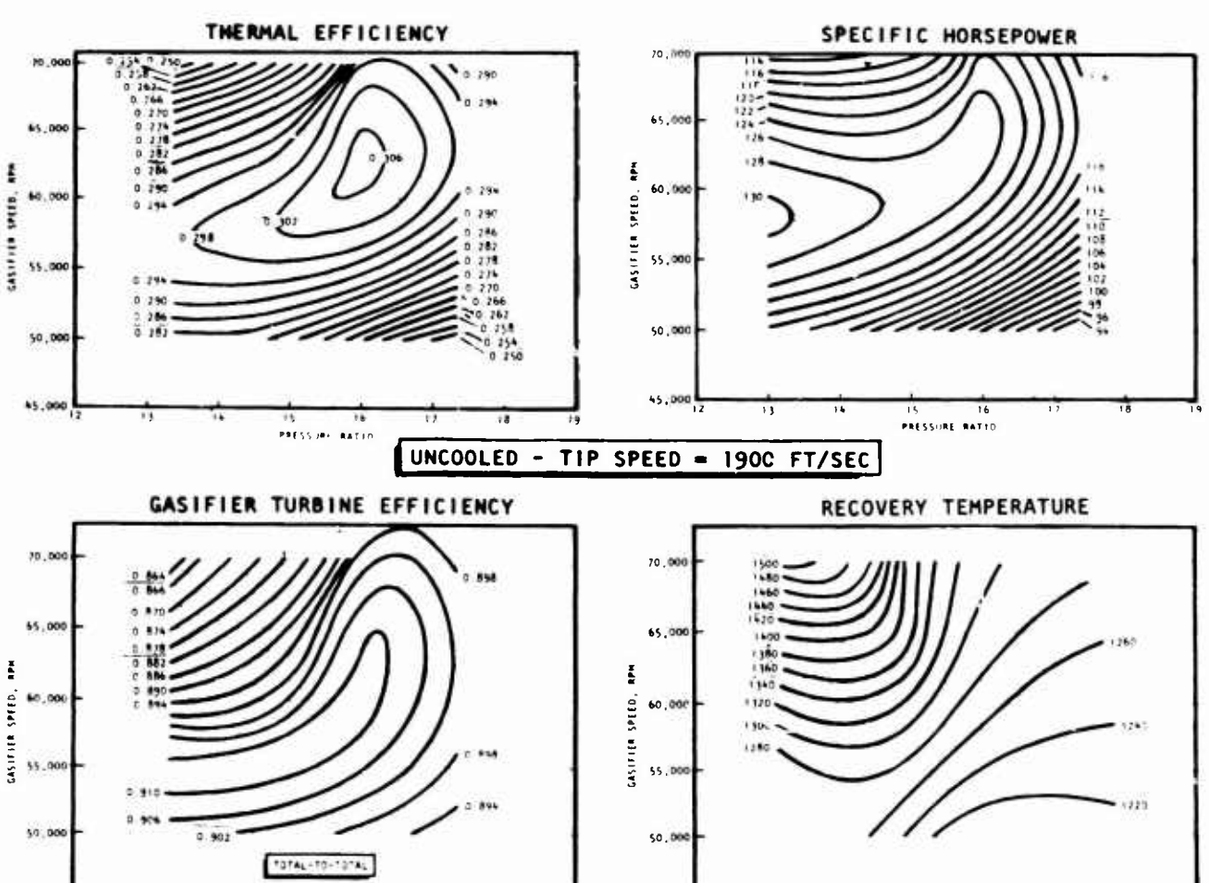

Figure 12. Engine Performance, 1700°F Inlet

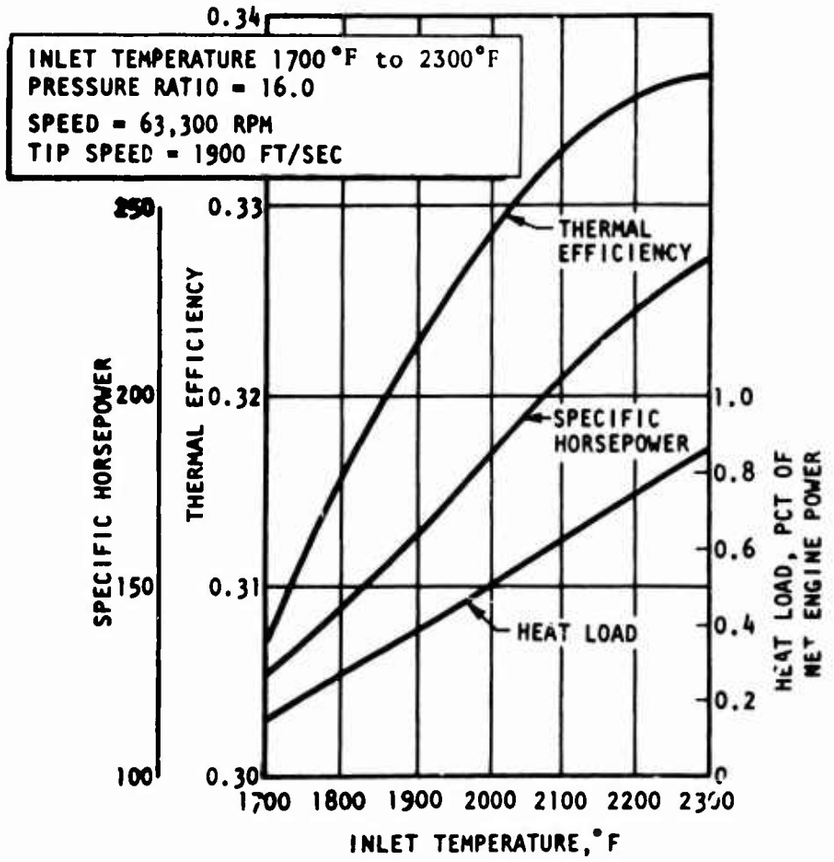

Figure 13. Inlet Temperature Effects

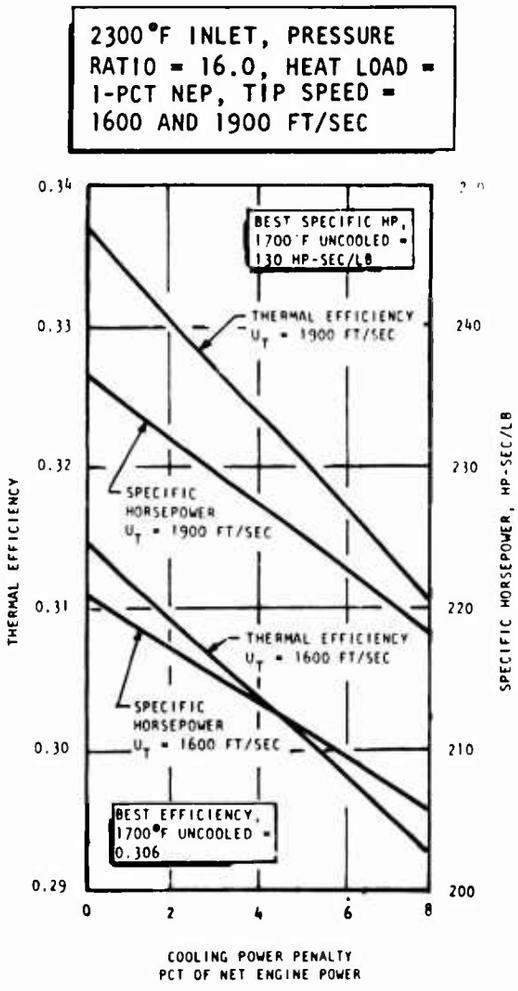

Figure 14. Cooling Effects

The effect of blade-root temperature on the optimum engine performance and design conditions is shown in Figure 15. As the temperature increases above 1200°F, the allowable stresses drop steeply and the blade annulus becomes increasingly smaller to stay within allowable stress limits. The effect of the decreasing annulus area may be seen also in the increasing Mach numbers relative to the rotor blade. This proceeds until the axial component of the absolute exit Mach number reaches unity and the annulus is choked. A further increase in temperature requires a reduction in rotative speed to stay within allowable stresses, because the annulus area cannot be decreased further. (Blade stress is proportional to $A_a N^2$.) The gasifier turbine efficiency remains about the same beyond the choking point, but specific power and thermal efficiency continue to decrease because of the effect of reduction in design speed on the compressor performance. Note that the blade relative inlet Mach number remains subsonic up to choking at exit.

These results are for untapered blades. With tapered designs, the root temperature levels are increased by about 150°F.

Pressure Ratio and Compressor Efficiency Effects

The effect of cycle pressure ratio, including a comparison of advanced and existing compressor performance, is shown in Figure 16. Both thermal efficiency and specific horsepower are seen to optimize at lower pressure ratios for the existing compressor, both with a loss of about 7 pct.

Tip Speed Effects

The effect of tip speed on overall performance may be seen in Figure 17. The optimum tip speed for the conditions shown was 2150 ft/sec, which was obtained without regard to stress limitations. Limiting the tip speed resulted in efficiency and power losses of 1.5 pct for 1900 ft/sec and 8 pct for 1600 ft/sec. An unexpected advantage of the higher tip speed is that even though the effective gas temperature is 100 degrees lower for 1600 ft/sec, the increased blade heights for optimum performance (greater heat transfer area) resulted in higher blade-root temperatures to maintain the same heat load. This shows that the effective heat transfer area is a very sensitive parameter, and measures to reduce this without severely penalizing performance would be beneficial.

Blade Heat Transfer Area Effects

It has been shown that the blade heat transfer area exposed to the hot gas is a very sensitive parameter which, if it could be reduced without severly penalizing turbine performance, would result in lowering the blade-root temperature and/or reducing the required level of cooling. This could be accomplished by using fewer or shorter blades, or by selecting the blade geometry (chord, solidity, thickness, etc.) to minimize the blade perimeter. All of these measures, however, involve tradeoffs with turbine performance and stress limits which could be evaluated only on an engine system basis, including the cooling power penalty; i.e., by optimization of the entire

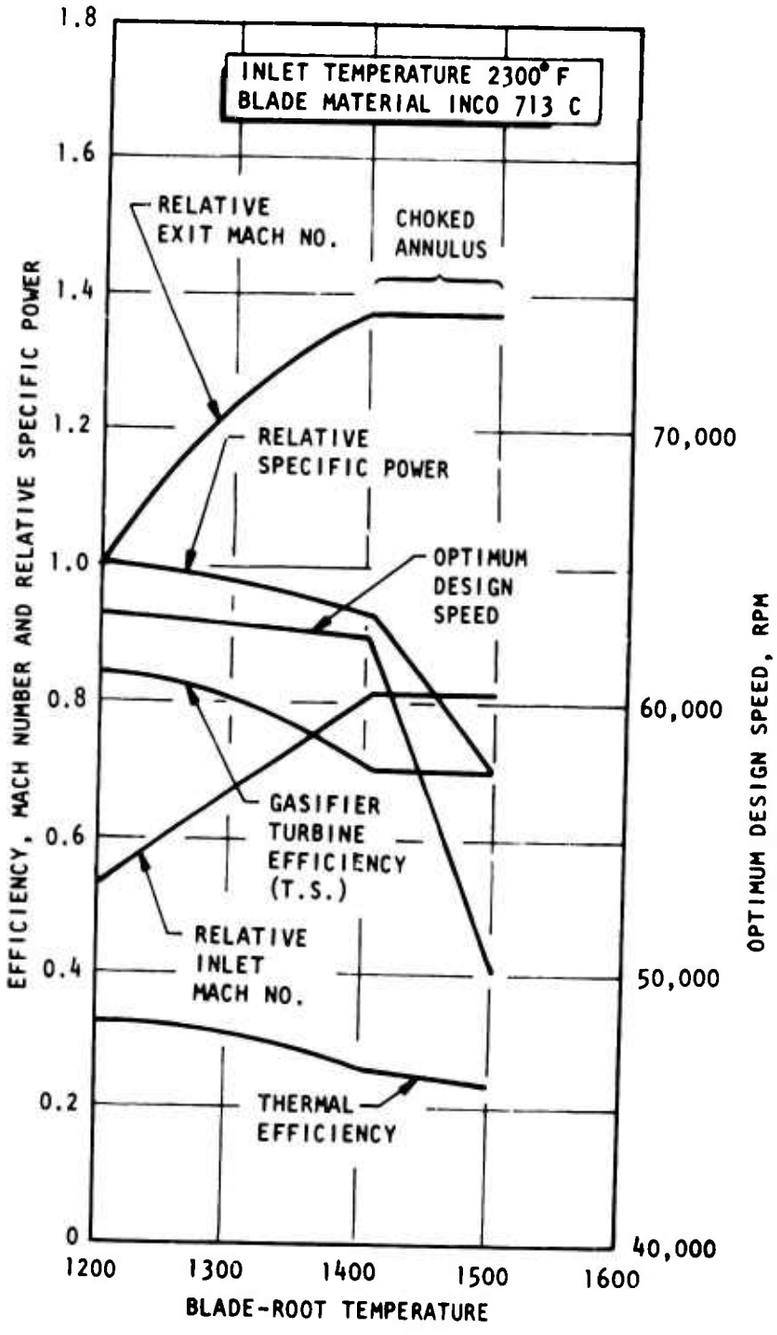

Figure 15. Blade Temperature Effects

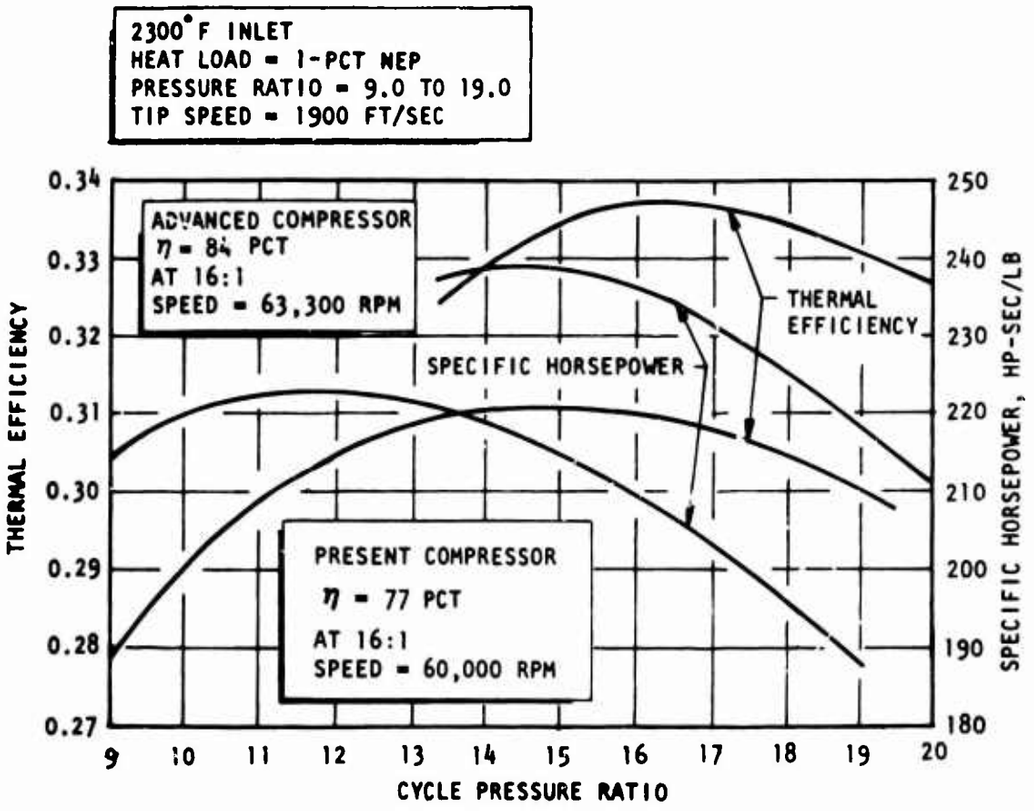

Figure 16. Pressure Ratio and Compressor Efficiency Effects

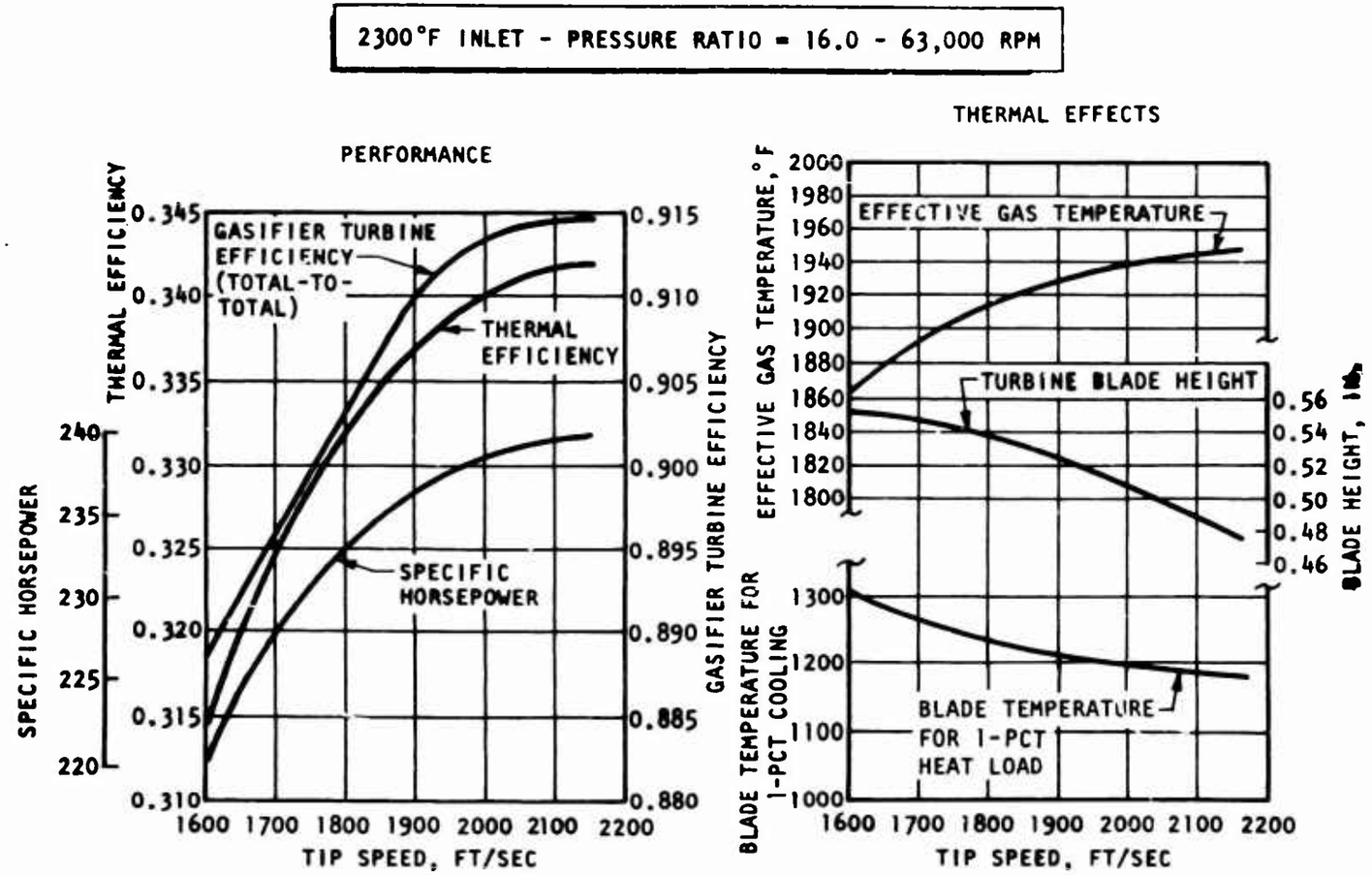

Figure 17. Tip Speed Effects

engine for maximum net output. Such a task would not be far beyond the capability of the present engine design analytical technique developed under this contract.

The use of fewer and/or shorter blades would probably be the most fruitful heat transfer approach. These, however, happen to be very sensitive with regard to turbine performance. The designs in this study are based on selection of blade spacing for optimum aerodynamic loading, which usually just precedes a sharp loss increase, as spacing is increased, because of flow separation. Some increase in spacing, however, could probably be tolerated with beneficial net engine effects.

GASIFIER TURBINE PERFORMANCE AND DESIGN

Performance

The achievable single-stage axial gasifier turbine efficiency as a function of cycle pressure ratio and rotative speed is shown in Figure 18, including the effect of compressor performance. At a tip speed of 1900 ft/sec, the effect of lower compressor performance is to shift the peaks to lower pressure ratios, but the total-to-total and total-to-static values remain fairly flat at 91.5 and 85 pct, respectively.

Another advantage of using a higher tip speed is seen in the comparison of exhaust energy in Figure 18. The exit velocity and swirl angle for optimum performance is much higher for 1600 ft/sec than for 1900 ft/sec, which results in higher duct losses.

Mach Number Effects

The rotor blade sonic conditions for the optimum designs may be seen in Figure 19. The relative inlet Mach number is a function of the stage pressure ratio, reaction, and tip speed, as shown for 2300°F inlet temperature in the upper left diagram. The fairly high optimum reaction levels result in subsonic relative inlet Mach numbers for all of the designs. The tip speed is most critical in increasing the inlet Mach number, since the highest levels, around 0.8, were obtained with the low tip speed (1600 ft/sec). Note that with turbine pressure ratios of 6:1, which were obtained at 1700°F inlet temperature, the inlet Mach number remains subsonic because of the reaction level.

Relative exit Mach numbers are a function of the degree of annulus restriction, as pointed out earlier, and are limited by the choking of the annulus (axial component of absolute exit Mach number unity). The optimum level of relative exit Mach number was between 1.0 and 1.2, with absolute exit Mach numbers entering the exhaust diffuser from 0.4 to 0.6.

With subsonic inlet and sonic or near-sonic exit conditions, the occurrence of supersonic velocities on the suction surface is virtually impossible to avoid. The detailed prediction of the weak shock phenomena and boundary layer interaction effects is very difficult in this regime, and no theoretical treatment is available in the literature. However, the problem has

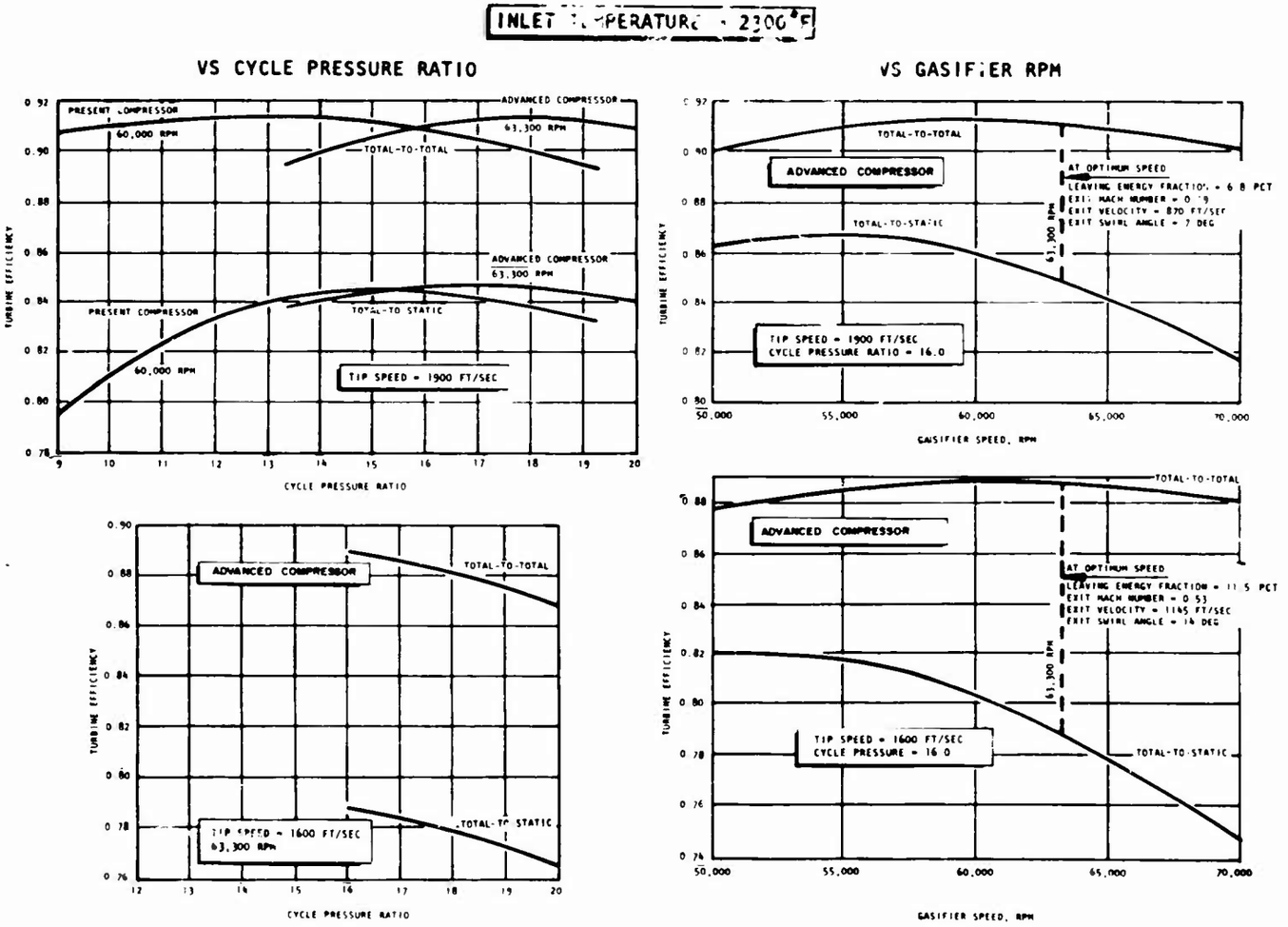

Figure 18. Gasifier Turbine Performance

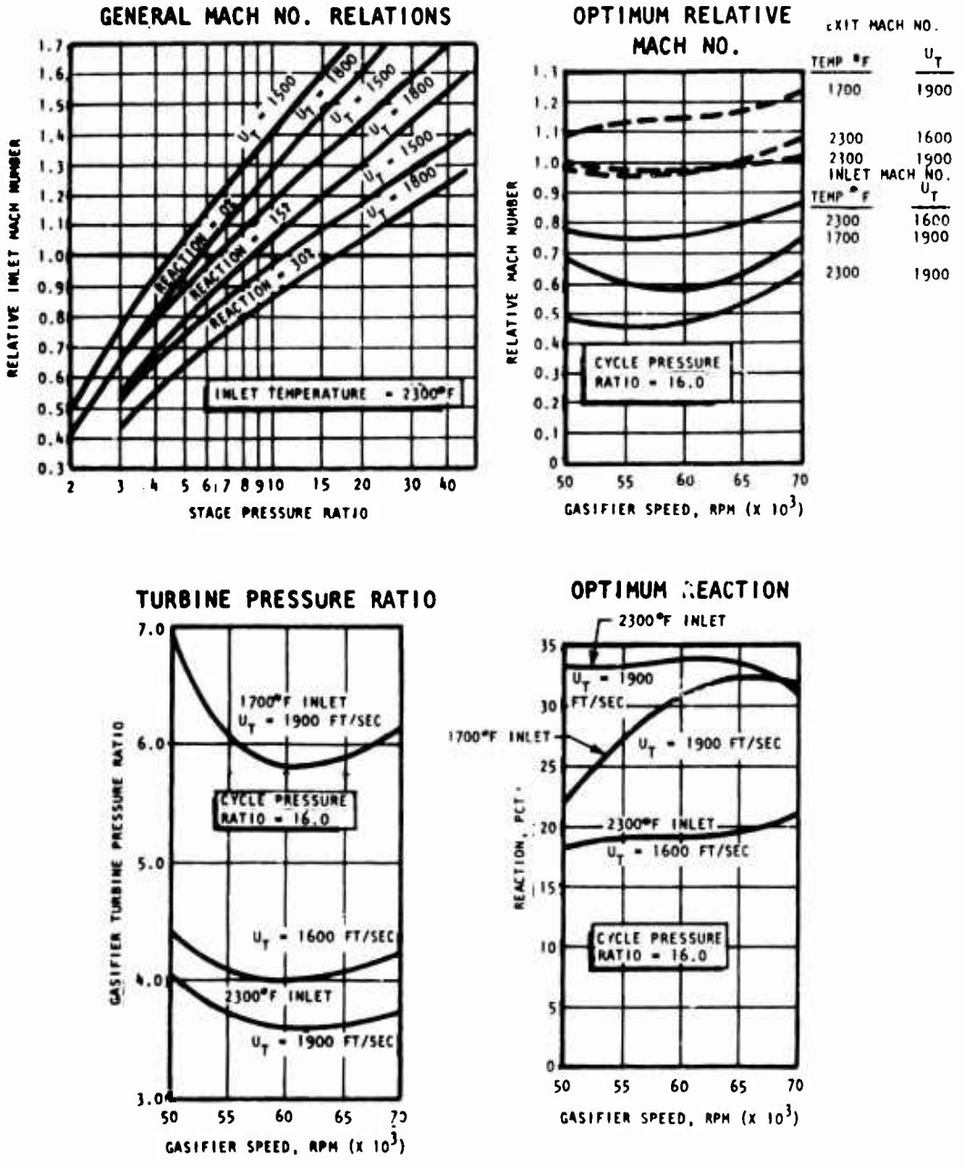

Figure 19. Gasifier Turbine Sonic Conditions

been approached experimentally by a number of authors, and the curve presented in Figure 20 from Reference 16 is widely accepted as being representative of the general trends. The curve shows a slight improvement in performance between 0.8 and 1.2 exit Mach number. This may be caused by local shock effects triggering early transition of boundary layers from laminar to turbulent so that the blades are less prone to separation losses.

The predicted improvement was not taken into account in the analysis, but it was concluded that the performance of gasifier turbine designs in the range of investigation would not be impaired by Mach number effects.

Design Characteristics

The variation of optimum gasifier turbine design characteristics with cycle pressure ratio, speed, and tip speed may be seen in Figure 21.

CONFIGURATION SELECTION

Upon completion of the generalized analysis, a gasifier configuration was selected at 2300°F inlet temperature, 16:1 compressor pressure ratio, and 63,000 rpm. This selection was made on the basis of the survey, which showed that the high temperature held promise of enough gain in specific power to make a detailed design study of cooling highly desirable. The compressor pressure ratio of 16:1 was just at the minimum specific fuel consumption (peak thermal efficiency). The maximum specific power occurred at a slightly lower pressure ratio, but on a rather flat curve, so that very little loss was incurred by the selection. Favoring the specific fuel consumption slightly seemed appropriate because the gain in SFC by increasing the inlet temperature would probably be consumed by the cooling penalty. The gasifier spool speed of 63,000 rpm was optimum for both specific power and SFC.

A slight change in the assumed compressor performance was made at the time of the configuration selection. A study of the compressor performance had disclosed that the initial "target" efficiency of 83 pct at 16:1 and 60,000 rpm would be very difficult to achieve with an in-line, two-stage, transonic-axial plus centrifugal combination. In agreement with the contracting agency, the target efficiency was downgraded to 80 pct under the same conditions. A value of 81 pct at 63,000 rpm was used as a basis for the selected gasifier configuration.

Design data for the selected gasifier turbine configuration is presented in Table I. The corresponding blade path and vector diagram may be seen in Figure 22. The distribution of losses for the selected design is shown in Figure 23. It will be noted that the predominant loss for both the nozzle and rotor is the profile loss.

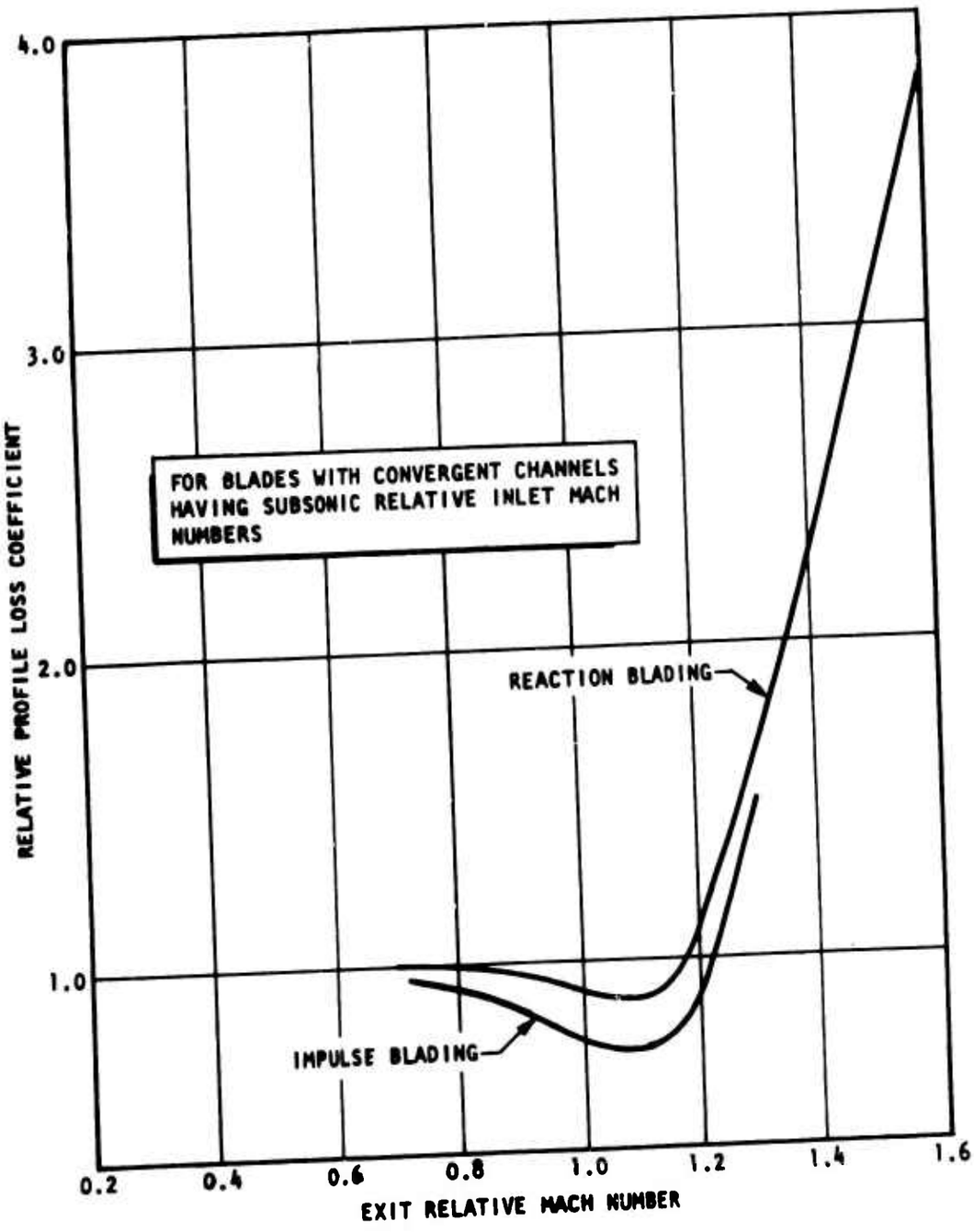

Figure 20. Losses Caused by Mach Number Effects

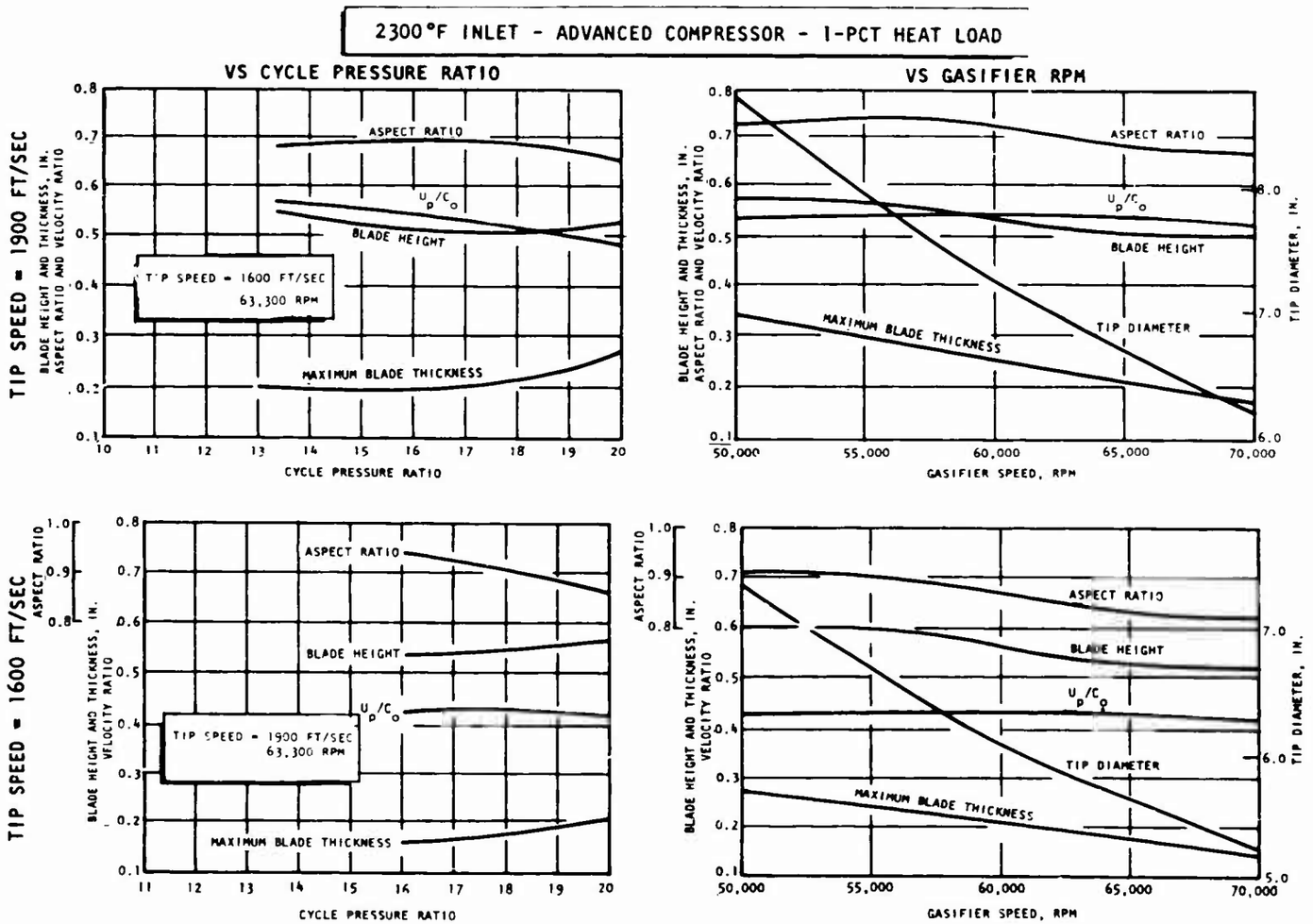

Figure 21. Gasifier Turbine Design Characteristics

TABLE I

SELECTED CONFIGURATION DESIGN DATA

Cycle Pressure Ratio	16.0
Turbine Inlet Temperature, °F	2300.0
Gasifier Speed, rpm	63,000
Turbine Tip Speed, ft/sec	1900
Inlet Total Pressure, psia	230.4
Exit Static Pressure, psia	59.3
Pressure Ratio	3.88
Δ h/T, Btu/lb R	0.073
Reaction	0.32
Pitch-Line Velocity Ratio (U_p/C_o)	0.533
Nozzle Exit Mach Number	1.2
Rotor Inlet Relative Mach Number	0.52
Rotor Exit Relative Mach Number	1.0
Specific Speed	60.2
Specific Diameter	1.46
Recovery Gas Temperature in Rotor, °F	1888
Blade-Root Temperature, °F	1200
Blade Centrifugal Stress (no taper), psi	43,447
Total-to-Total Efficiency, pct	91.5
Total-to-Static Efficiency, pct	84.1
Gasifier Turbine Shaft Power, hp	1310.0

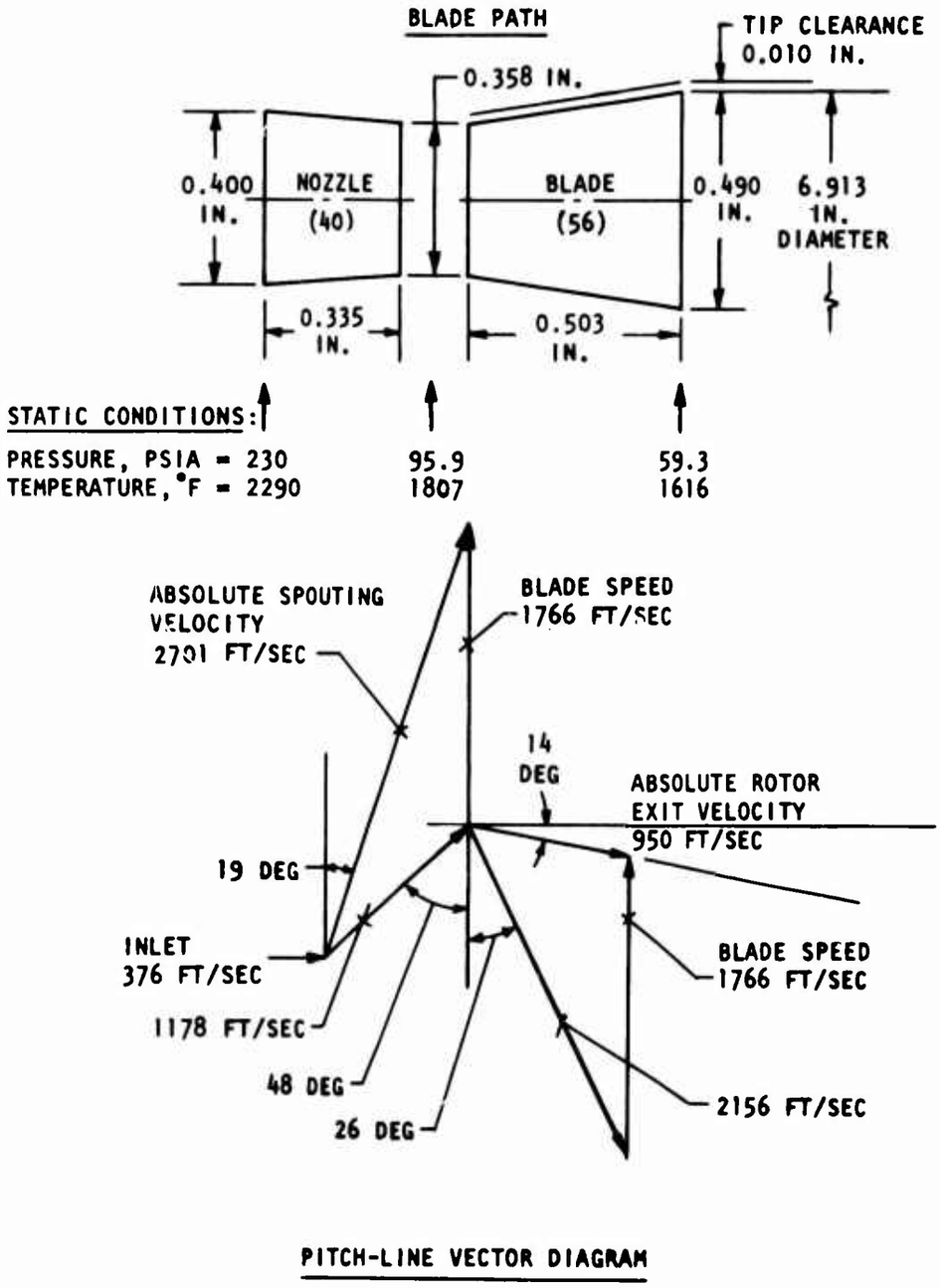

PITCH-LINE VECTOR DIAGRAM

Figure 22. Selected Gasifier Turbine Stage Design

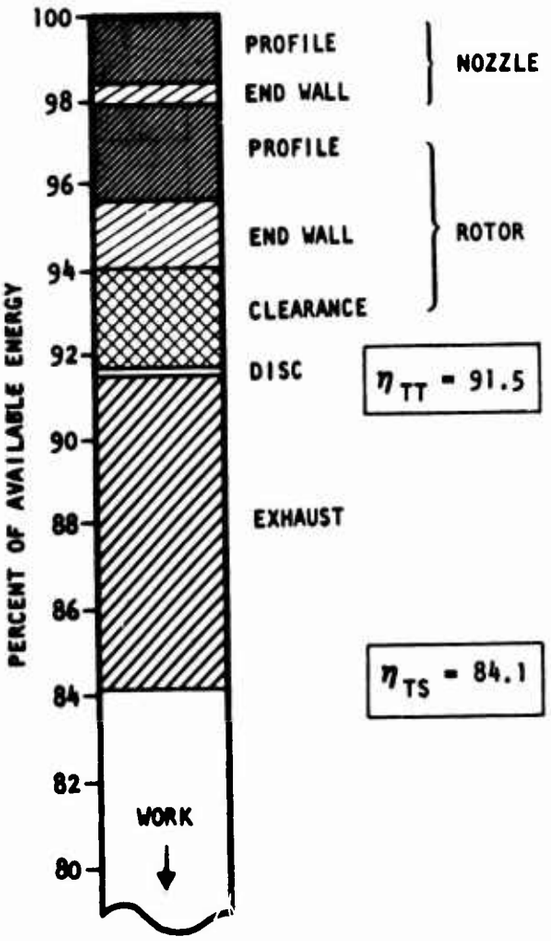

Figure 23. Distribution of Losses

DETAILED ANALYSIS OF THE SELECTED CONFIGURATION

AERODYNAMIC DESIGN

The relations of Bolte (Reference 4) were used in developing an efficient mean rotor blade profile. Bolte's relations for stagger angle and solidity had already been used in the turbine optimization code to establish the general stage design with regard to blade spacing and chord length. The rest of the details were established using relations from the reference for maximum thickness, location of maximum thickness, maximum camber, location of maximum camber, and thickness distribution. Bolte's relations are based on an extensive survey of cascade data and provide a general correlation of efficient profile design characteristics as functions of the vector angles.

The resulting mean rotor blade profile is shown in Figure 24. The trailing-edge thickness was increased to 0.040 inch from the previously assumed 0.020 inch, to allow for the cooling passage design.

Because of time limitations, the sections for the hub and tip were not designed. Although they would actually involve slightly different shapes and blade angles because of the turbine vortex, it was considered that the use of one basic shape would be sufficiently accurate for the heat transfer and stress analysis.

A calculation of the mean velocity distribution for the profile, using the graphic compressible technique described in Reference 8, was then performed. The resulting velocity distribution is shown in Figure 25.

DETAILED HEAT TRANSFER ANALYSIS

Cooling Details

The internal passage design of the cooled rotor blade is shown in Figure 26. The cooling air enters the blade through the central insert and is discharged through two slots, 0.007 inch in width, so as to impinge against the inner surface of the leading edge. From there it flows back along the blade inner surfaces and leaves the blade through the trailing edge. It is believed that manufacture of such a blade would be practical using investment casting techniques similar to that of Reference 10. Such castings are also described in Reference 3.

The design of the insert and integrally cast end-closure will be described in detail in the Stress Analysis section. The end-closure is deeply inset near the leading edge, leaving the forward tip of the blade hollow and exposed. This was found in the heat transfer analysis to be the optimum arrangement for cooling. The forward leading-edge tip was sufficiently cooled by conduction, and the reduction of the internal flow-passage height lightened the insert and improved the internal convective heat transfer. The pedestals in the internal passage provide improved heat transfer by extending the hot surface into the cooling air stream. They also permit an effectively wider cooling passage than could otherwise be used, because

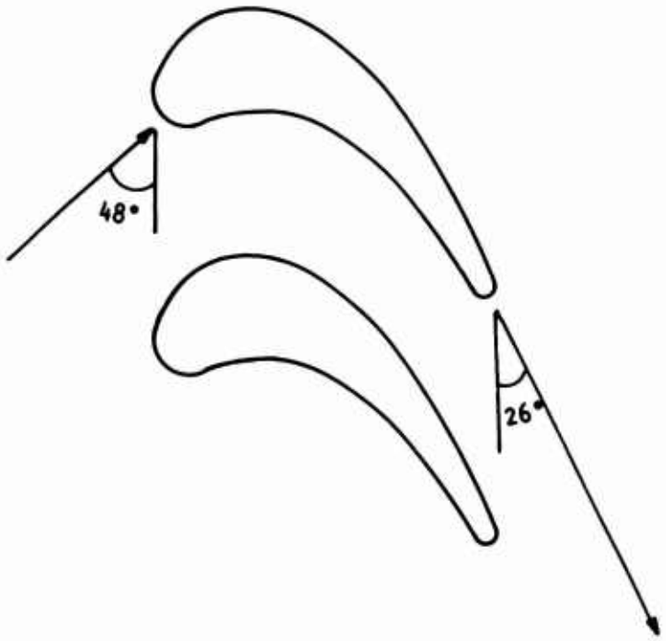

CHORD = 0.598 IN.
PITCH = 0.360 IN.
MAXIMUM THICKNESS = 0.163 IN.
LEADING-EDGE RADIUS = 0.049 IN.
TRAILING-EDGE THICKNESS = 0.040 IN.
NO. BLADES = 56

Figure 24. Mean Rotor Blade Profile

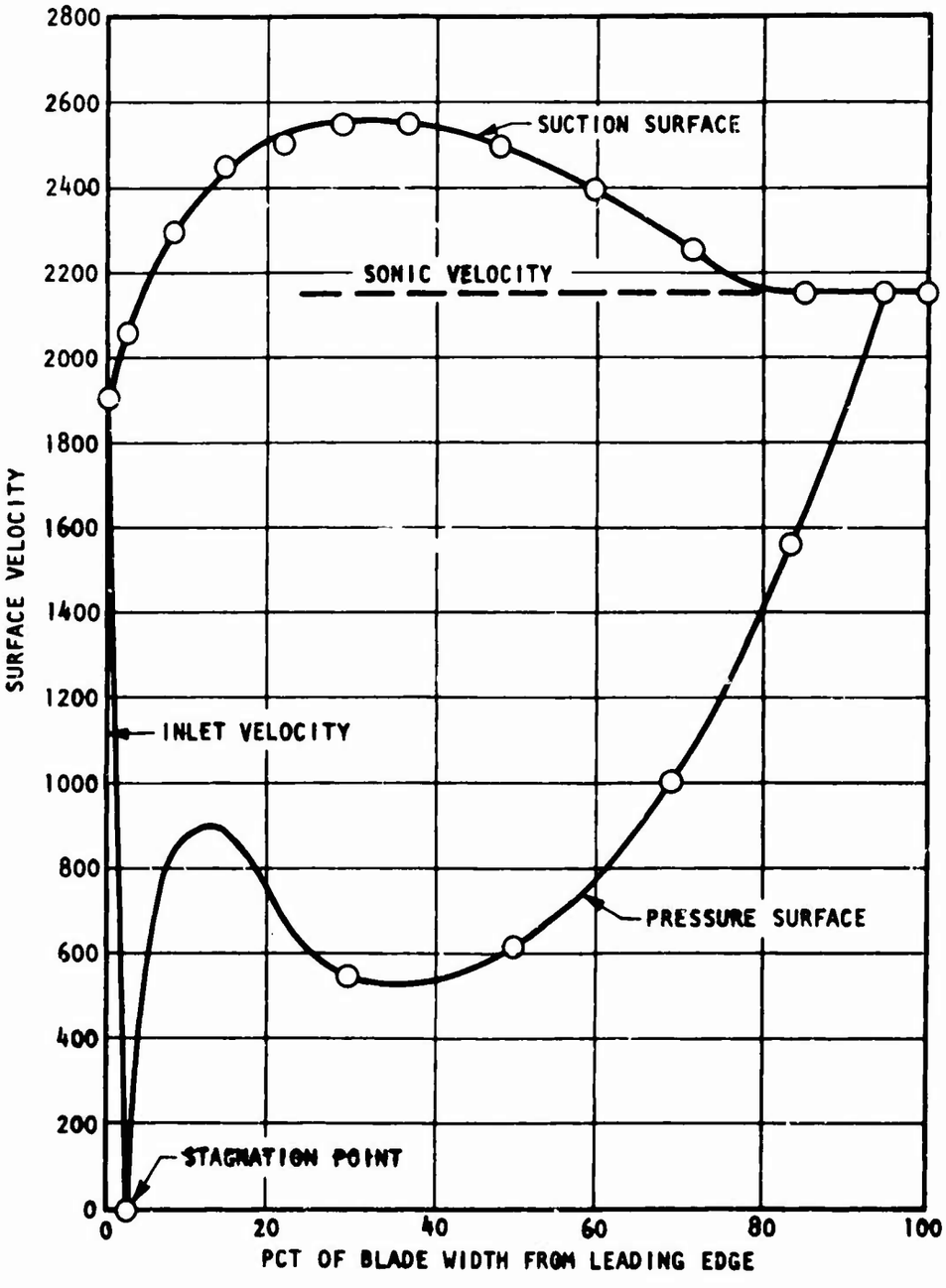

Figure 25. Rotor Blade Profile Velocity Distribution

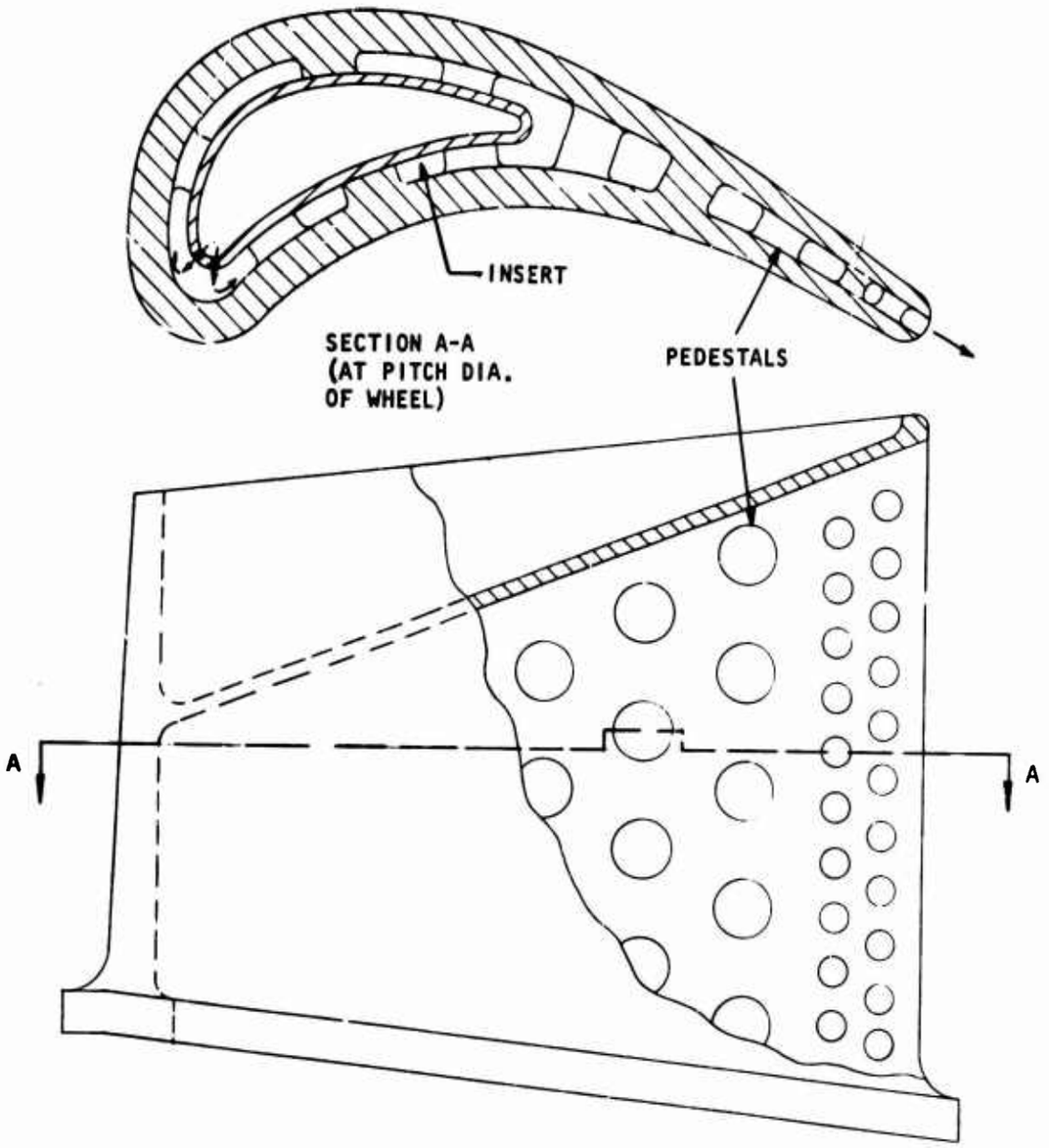

Figure 26. Air-Cooled Blade Design

they restrict the flow area, thus keeping the velocity high. This may facilitate manufacture since narrow passages are more difficult to cast.

Method of Analysis and Results

The distribution of external hot-gas temperatures is shown in Figure 27. These temperatures were calculated from the previously described profile velocity distribution. Local external heat transfer coefficients were calculated according to the following relations (Reference 6):

Laminar

$$N_{ux} = 0.332\ P_r^{1/3}\ R_{ex}^{1/2}$$

Turbulent

$$N_{ux} = 0.0296\ P_r^{1/3}\ R_{ex}^{0.8}$$

where

N_{ux} = Nusselt number, based on surface length from stagnation point, and local gas properties

P_r = Prandtl number of hot gas

R_{ex} = Reynolds number

The laminar-to-turbulent boundary layer transition was assumed to occur at a surface-length Reynolds number of 60,000. The transition point depends on the degree of turbulence (free-stream), which must be estimated, but data in Reference 17 indicated that the assumed transition point was reasonable.

The resulting local external heat transfer coefficients are shown in Figure 28.

The internal cooling airflow was based on a technique of injection through the outer turbine wheel and blade root, utilizing the side of the turbine wheel as a cooling air compressor by means of vanes integral with the wheel. Calculations for this system showed that cooling air would be provided at the insert in the blade at 180 psia and 860°F, accounting for compression, friction loss, and heat transfer enroute, if the source of cooling air is taken within the radial compressor stage at a pressure of 108 psia.

The compressible flow and velocity distribution inside the blade were calculated, based partly on the estimated minimum castable passage dimensions, and accounting for friction loss, heat transfer, and area-change effects. The flow passage was designed so as to provide about 700-ft/sec impingement velocity at the leading edge. Under these conditions, the

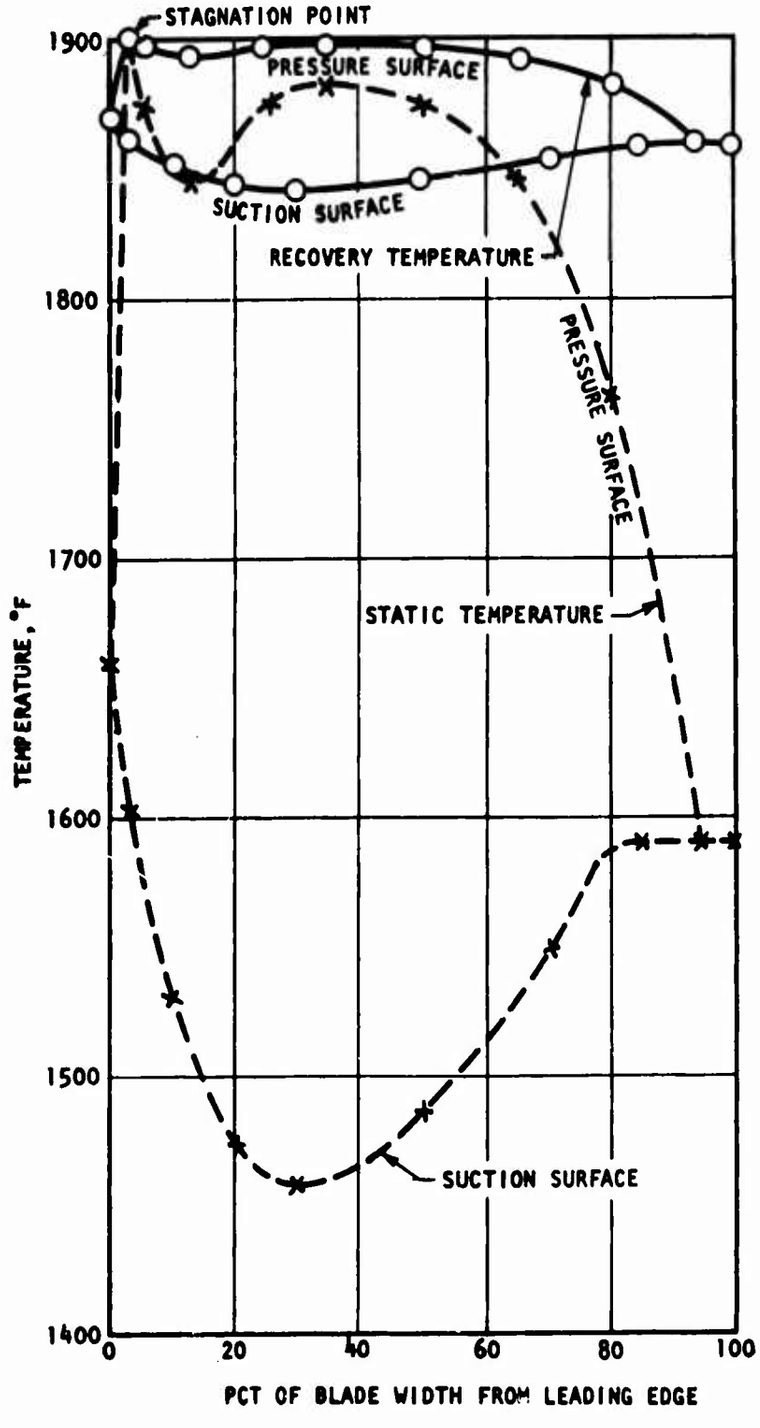

Figure 27. Rotor Blade Profile Temperature Distribution

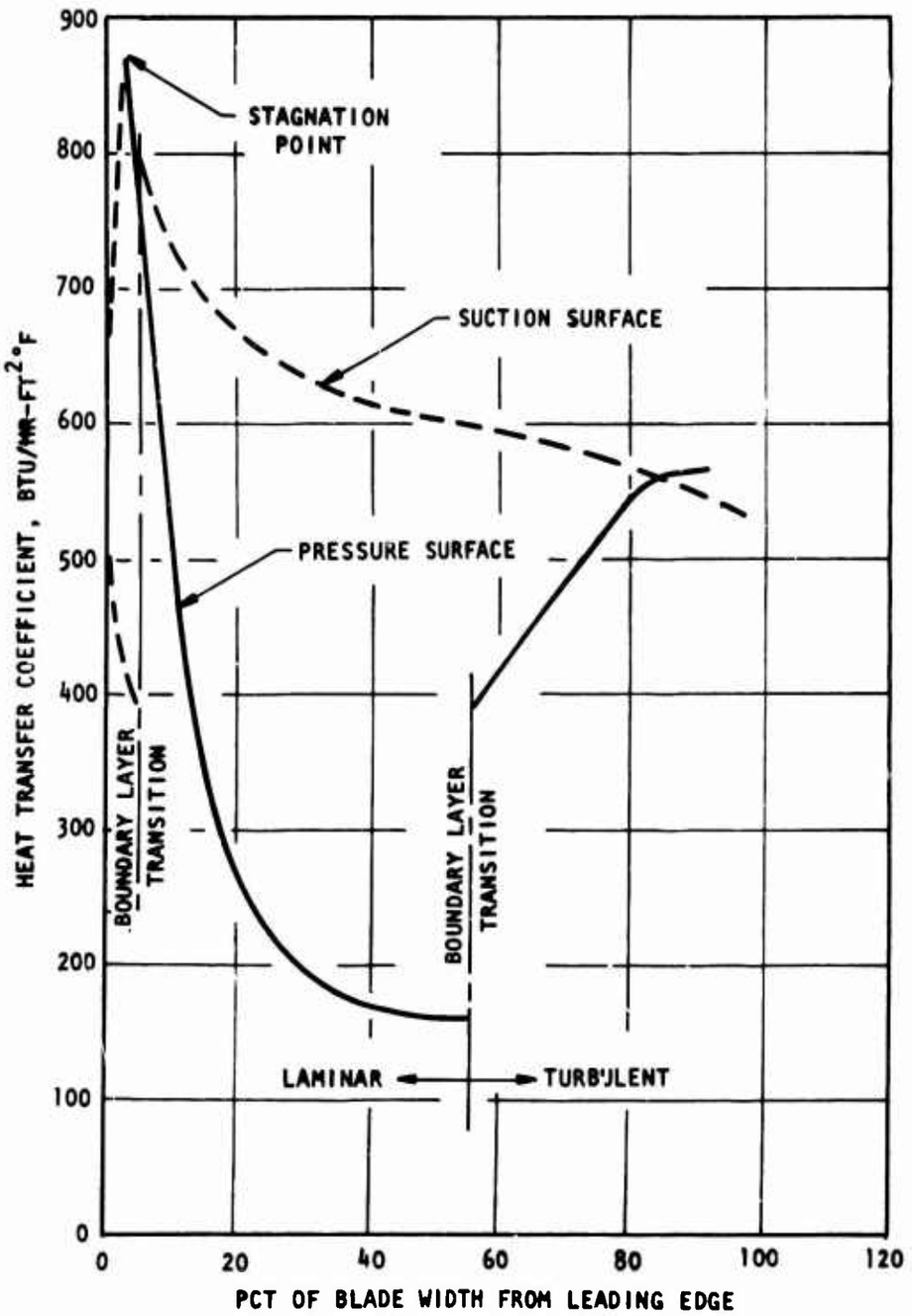

Figure 28. Rotor Blade Profile External Heat Transfer Coefficient Distribution

cooling flow would be choked at the trailing-edge slot at the level of external pressure (59.3 psia). The calculated maximum mass flow for all rotor blades was 0.31 lb/sec, or 6.2 pct of compressor airflow. Nozzle cooling is accomplished separately by burner-bypass, and therefore does not involve a parasitic flow loss.

Using the calculated internal velocities, heat transfer coefficients were calculated as follows:

Impingement (Reference 14)

Laminar Flow:

$$h = 0.906\, k\, P_r^{1/3} \sqrt{\frac{U}{Wv}}$$

where

h = heat transfer coefficient, $\frac{\text{Btu}}{\text{sec-in.}^2\text{-°F}}$

k = air thermal conductivity, $\frac{\text{Btu}}{\text{sec-in.}^2\text{-°F}}$

P_r = Prandtl number

U = jet velocity at wall, ft/sec

W = effective jet width, ft

v = kinematic viscosity, ft^2/sec

Convective Passage (Reference 6)

Turbulent Flow:

$$N_{ud} = 0.0243\, P_r^{1/3}\, R_{ed}^{0.8}$$

where

N_{ud} = Nusselt number, based on hydraulic diameter

P_r = Prandtl number

R_{ed} = Reynolds number, based on hydraulic diameter

The internal passage temperatures, velocities, and heat transfer coefficients are shown in Figure 29. By comparison with Figure 28, it may be seen that the internal heat transfer coefficients are roughly the same order of magnitude as the external values.

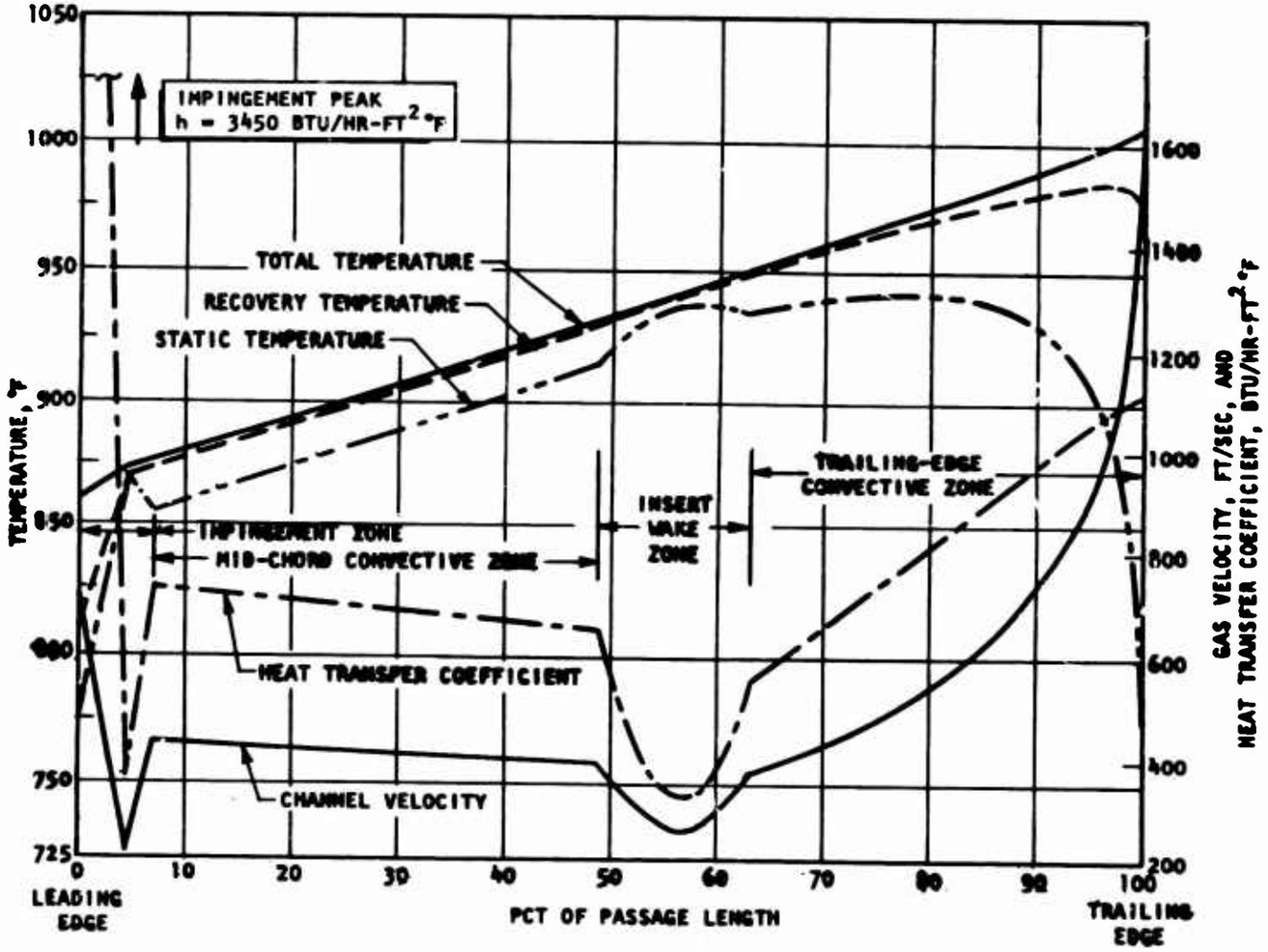

Figure 29. Blade Cooling Air Internal Temperature, Velocity, and Heat Transfer Coefficient Distribution

The foregoing calculated internal and external temperatures and heat transfer coefficients were used in a three-dimensional digital computer network model of the blade to find the steady-state temperature distributions. The optimum distribution in conjunction with blade strength requirements was found by several trials involving changes to the internal passage vertical shape. The resulting temperature distribution is shown in Figure 30.

The total heat flux removed through the blade walls was 18 Btu/sec. This amounts to a 2.2 pct of the net engine power. The average blade-root temperature was 1370°F. Note that the root temperature is hotter than the adjacent material just above it because of the fin effect of the platform.

STRESS ANALYSIS

A detailed layout of the blade and attachment design is presented in Figure 31. This design features an attachment involving a double-straddle fir-tree root; i.e., straddled in both the blade and the disc. The blade construction may be seen in the isometric sketch in Figure 31. This arrangement has a number of advantages.

1. It permits the casting to be cored from the base, thus allowing the tip closure to be integrally cast with the blade.
2. It permits an insert to be inserted and locked at the base, thus eliminating insert fabrication and attachment problems.
3. The space between the root halves may be used as the circumferential cooling air manifold, thus utilizing space and material effectively, so that no structural "deadweight" problem exists.

The blade section has been set back on the root so as to allow assembly of the insert. Blade locking and sealing of the fir-tree edges is accomplished by rivets and plates around the periphery, as shown in the isometric sketch in Figure 31.

Blade Centrifugal and Bending Stress

The decision was made to use IN-100 for the blade material because of its high rupture strength in the temperature range of 1200 to 1400°F. Because IN-100 is a castable material, it lends itself readily to this application.

The blade was tapered to reduce the centrifugal stress. The tip section area was 62 pct of the root section area.

Blade section properties were calculated using computer codes, based on the detailed section coordinates. Power bending stress was based on a tangential loading of 7.29 lb/blade and an axial pressure differential of 50 psi.

The average combined centrifugal and bending stress vs blade height is shown in Figure 32. Stresses are based on a nominal speed of 63,000 rpm and include a 10-pct overspeed factor and a blade-root stress concentration factor of 1.3. The increase in stress just below the 3.1-inch radius is

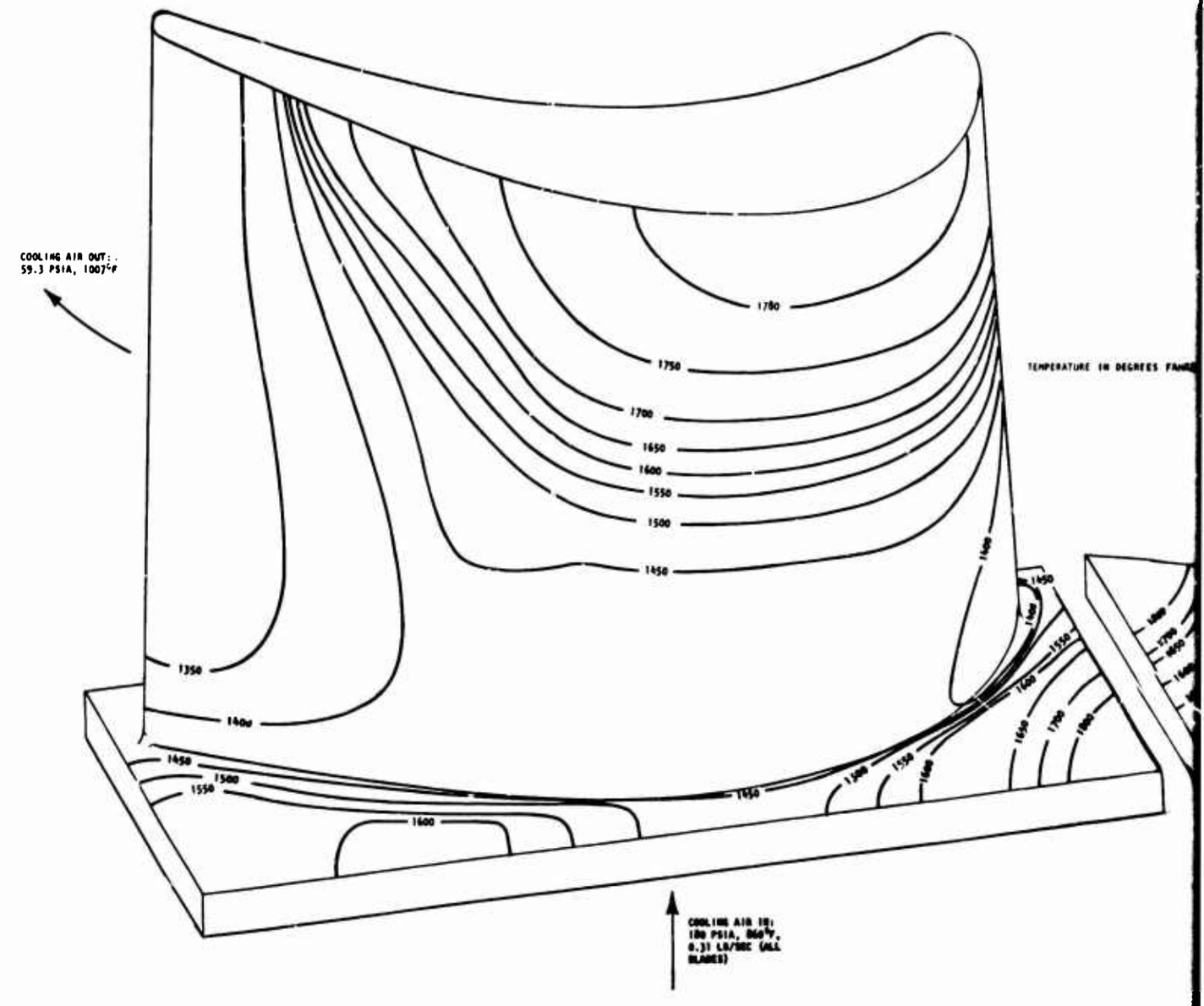

Figure 30. Blade Temperature Distribution

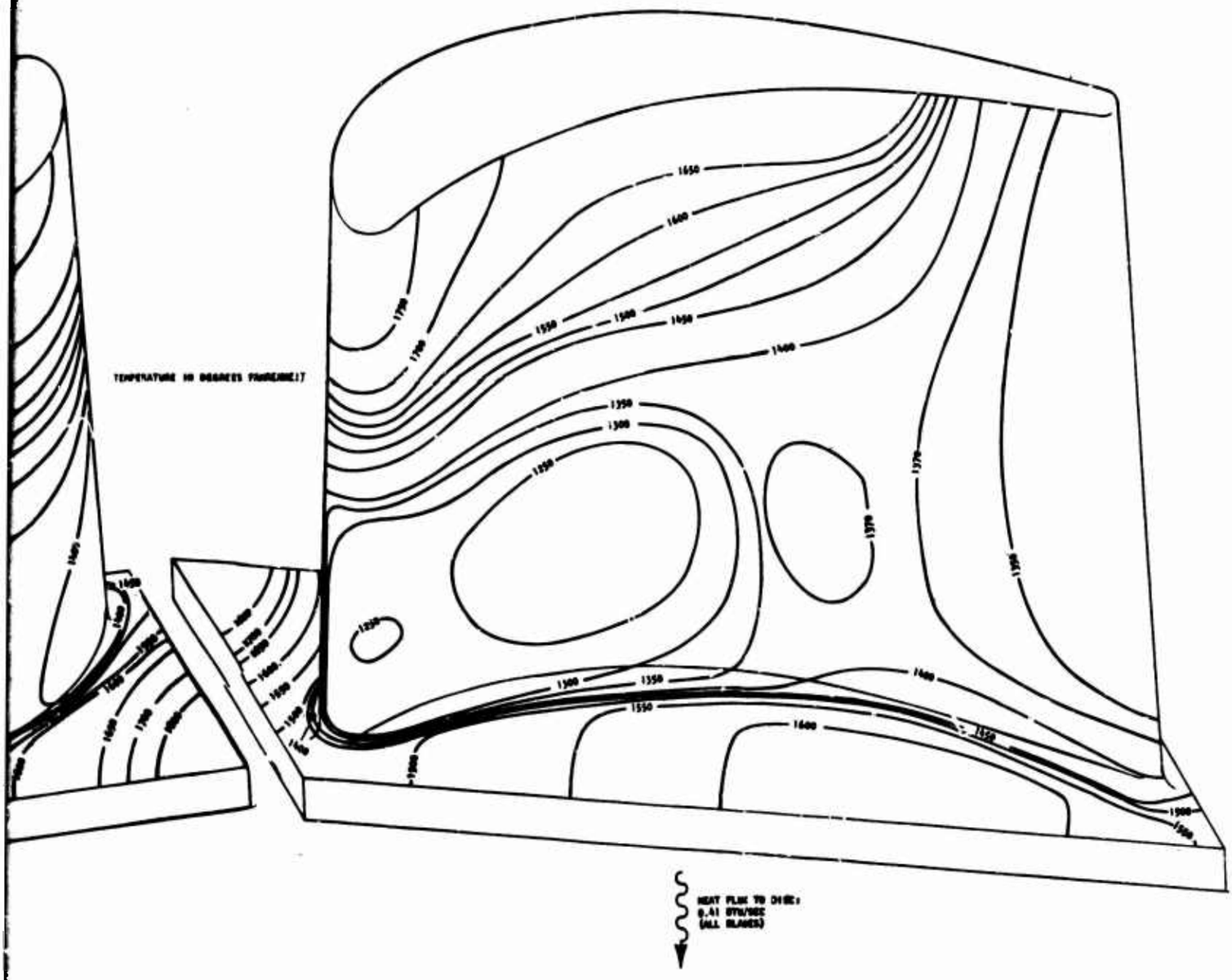
TEMPERATURE IN DEGREES FAHRENHEIT
1650
1600
1550
1500
1450
1400
1350
1300
1250
1200
1150
1100
1050
1000
950
900
850
800
750
700
650
600
550
500
450
400
350
300
250
200
150
100
50
HEAT FLUX TO DISC:
0.41 BTU/SEC
(ALL BLADES)

B

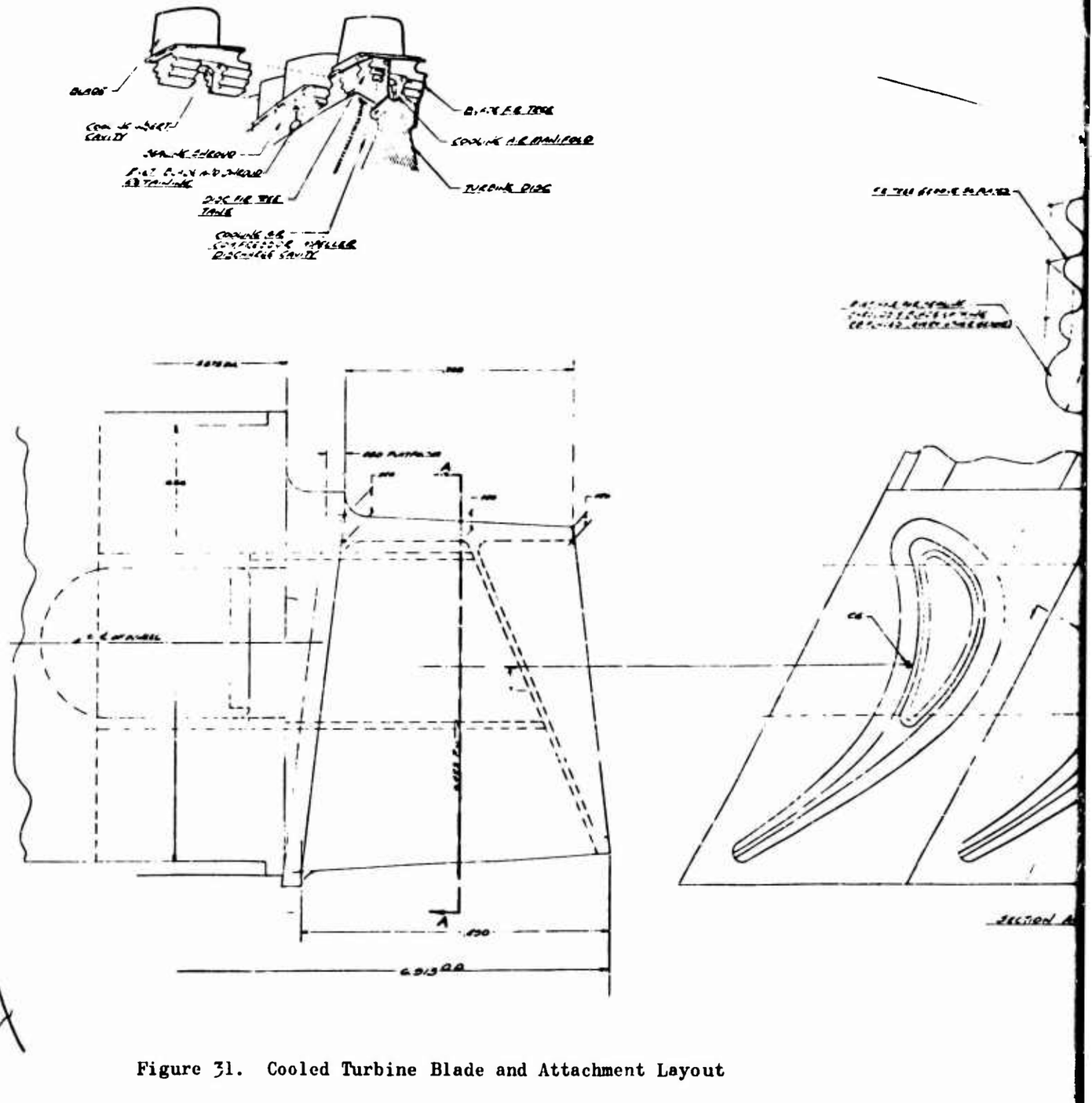

Figure 31. Cooled Turbine Blade and Attachment Layout

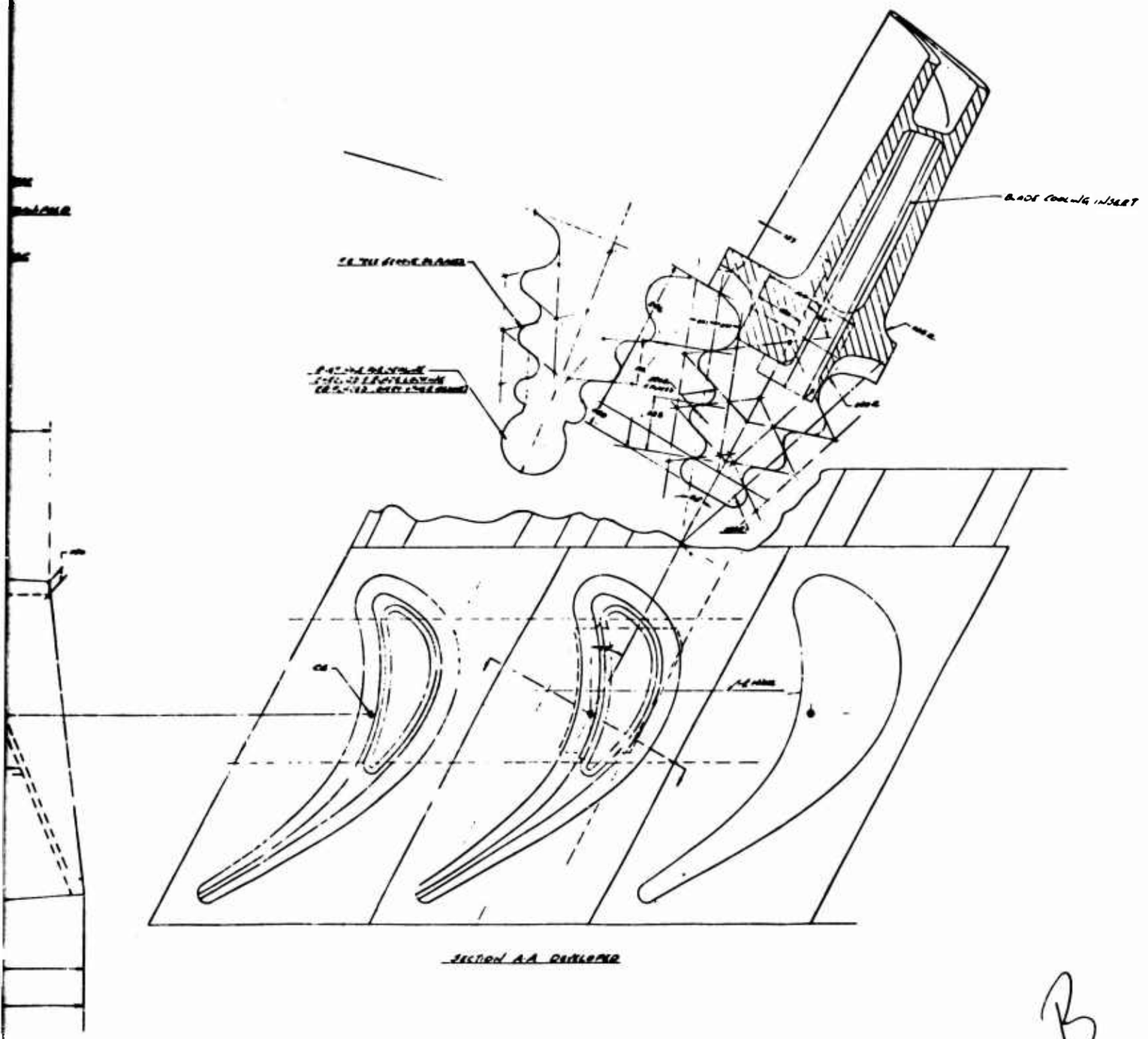

SECTION AA DEVELOPED

B

Attachment Layout

due to the latter. The tip closure shown in Figure 32 was used in the stress calculations, although in the final design the closure was recessed down into the blade. The stress analysis was not repeated because it is slightly conservative to assume that the closure is at the extreme tip.

The required minimum 100-hour rupture strength for safety and the available strength for IN-100, based on the average radial temperature distribution from Figure 30, show that the blade is satisfactory as designed.

Preliminary Vibratory Analysis

Blade frequencies were calculated based on cantilever bending deformation and are summarized in Figure 33. This type of frequency calculation is preliminary and serves only as an indication of possible blade frequencies. Based on these preliminary calculations, the operating speed range from 40,000 rpm to 70,000 rpm is free from serious resonance. Further analysis and testing of actual blade hardware will be required to define the blade frequencies more accurately. If this results in blade resonant frequencies within the desired operating speed range, minor blade or nozzle geometry changes would be made.

Attachment Stress

The fir-tree stresses are shown in Figure 34. All stresses are based on a nominal speed of 63,000 rpm and include a 10-pct overspeed factor and a stress concentration of 1.1. The fir-tree design has not been balanced or toleranced for final design detail, but the design shown here is feasible.

Disc Stress

The disc stress and temperature distribution may be seen in Figure 35. The design of the disc is such as to provide a burst speed of 135 pct of the operating speed, as described in the discussion of ground rules for the generalized analysis. This margin may be seen by the comparison of stresses and strength shown in the figure. The detailed optimized design and analysis included both thermal and centrifugal loads. The comparison of the actual and the theoretical analysis shapes in Figure 35 shows that the actual design is conservative because the effective rim diameter is smaller.

Also shown in Figure 35 are the locations of the cooling air inlet holes, which are placed so as not to compromise the disc structural design. The holes are located under the blades above the neck so as to avoid high stress regions in the neck and under the disc fir-tree tangs. The holes are located on every other slot so that one hole feeds two blades. Alternate slots are used for the blade locking and sealing plate rivets. These arrangements may be seen in more detail in Figure 31.

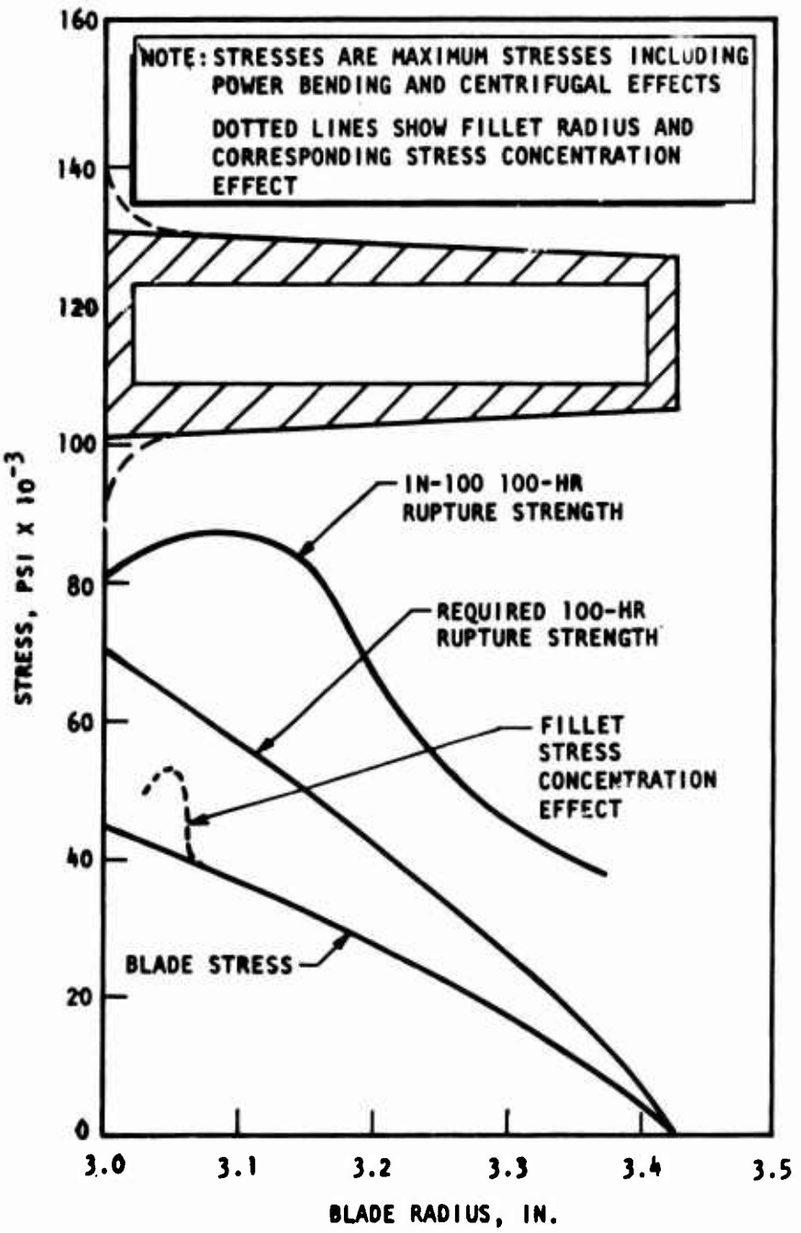

Figure 32. Blade Centrifugal and Bending Stress

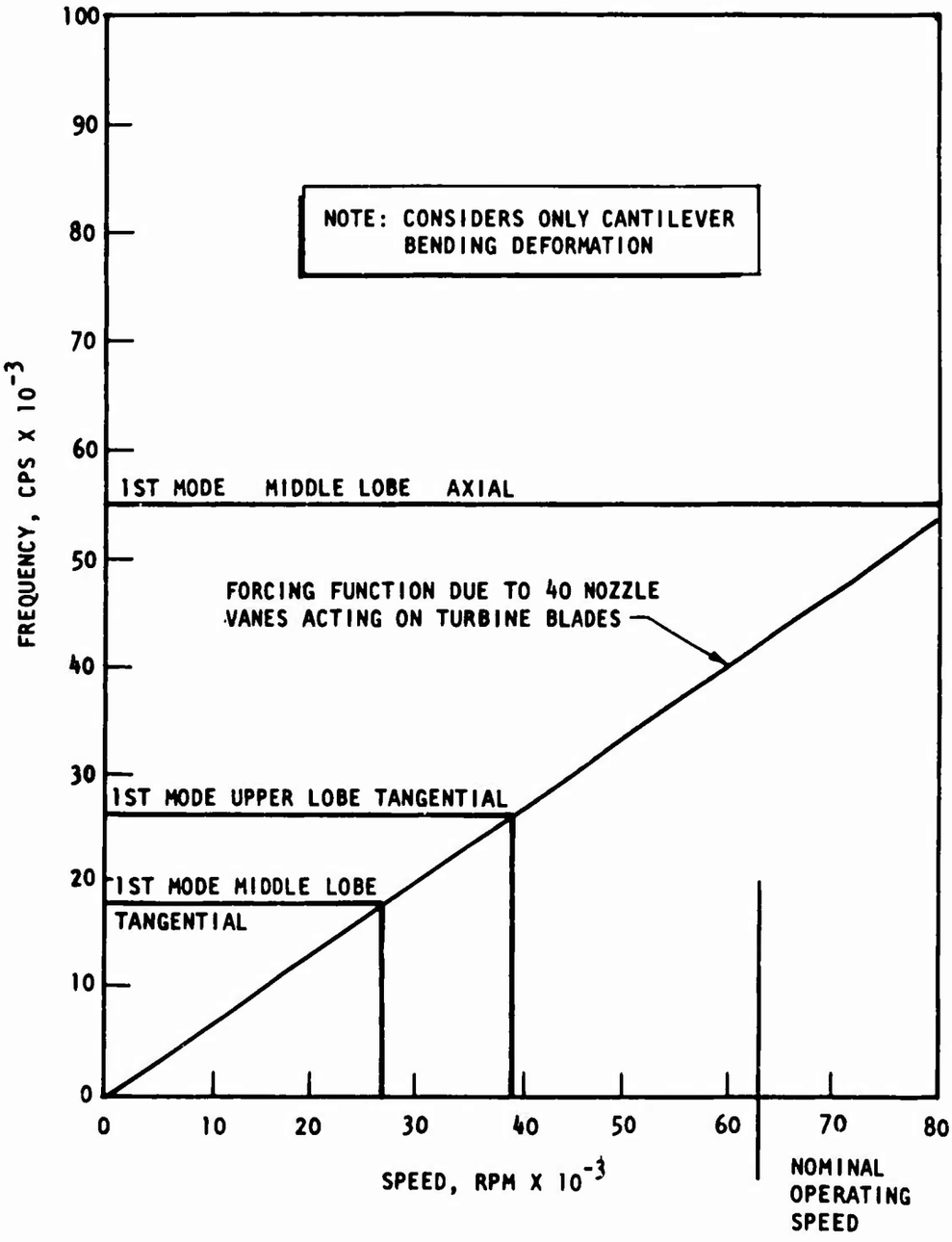

Figure 33. Turbine Blade Resonance Diagrom (Frequency vs Speed)

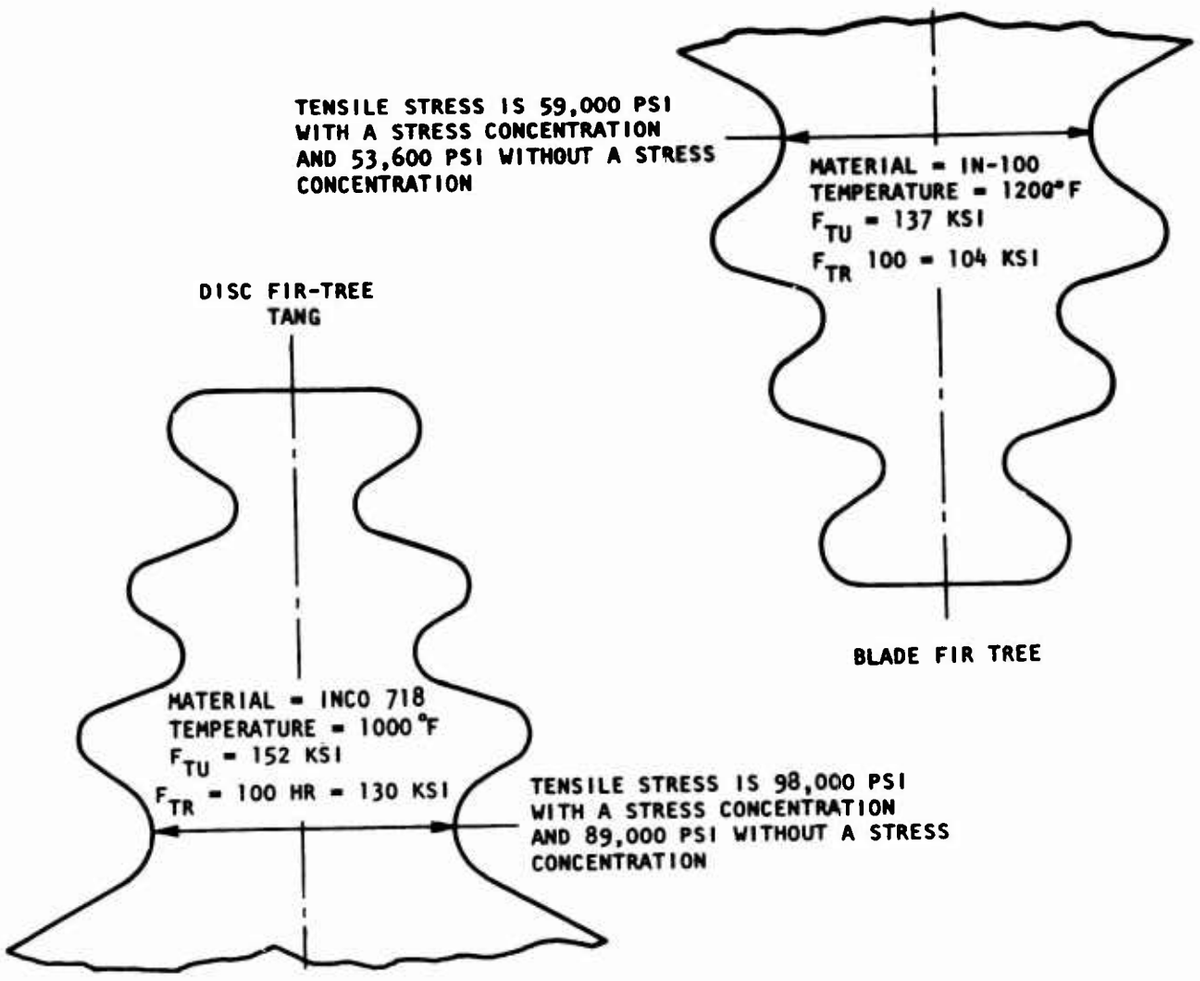

Figure 34. Stresses in Fir-Tree Configuration

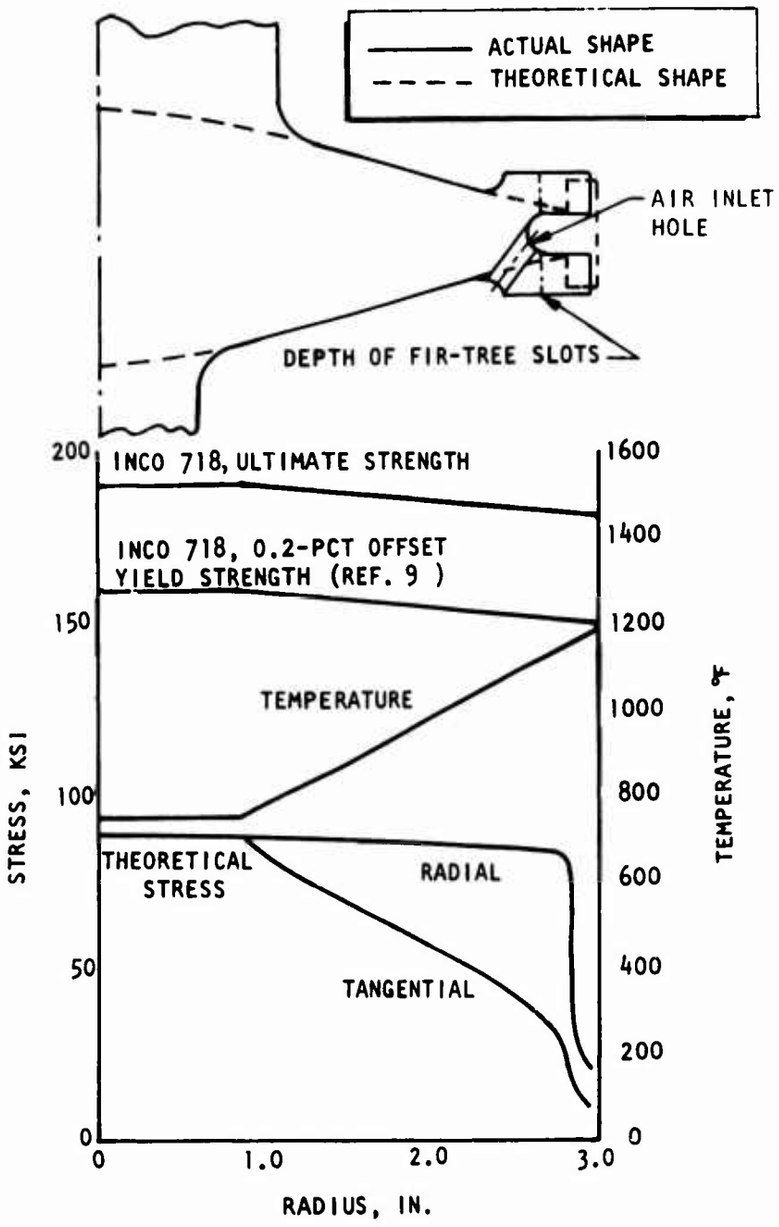

Figure 35. Disc Temperature and Stress Distribution

DESIGN LAYOUT

A scale layout of the selected design configuration is presented in Figure 36. Dimensions have been omitted for clarity. The attempt has been to show as clearly as possible the relation and practical integration of the gasifier turbine unit with other components of the engine. However, the configurations of the burner, compressor, and other components external to the gasifier turbine and cooling air supply system are approximate and are intended to represent a typical arrangement.

The two-stage power turbine shown is based on a design speed of 28,000 rpm. Lower speeds would require larger diameters.

The flow of the primary compressor air is shown by the heavy arrows in Figure 36. Nozzle cooling is accomplished by using bypassed compressor air obtained by balancing the burner air intake to provide sufficient pressure drop through the nozzles for adequate cooling. If this causes unsatisfactory burner performance or excessive pressure loss, cooling of the nozzles can be effected by discharge of air through the nozzle vane walls into the hot-gas stream, as must be done in the rotor. This, however, is an inherently less effective way to cool than the regenerative bypass arrangement.

The fine arrows in Figure 36 show the flow of rotor cooling air in a cooling system designed by the contractor. The attractive features of this system are the "side-wheel compressor" method of injecting air into the rotor without compromising the disc structural design, and the "double-straddle fir-tree" attachment technique which allows a very efficient attachment structural design and integral casting of the blade tip closure.

The source of the cooling air in this system is within the radial compressor stage at 108 psia and approximately 525°F. This air is piped externally to a manifold at the OD of the power turbine nozzle assembly. Two diametrically opposed pipes are used to reduce the size of the manifold. The pipes and manifold are sized for 300 ft/sec average velocity, which should keep the pressure loss to a sufficient minimum. A pressure loss of 10 pct between the source and the side-wheel compressor intake was used for the cooling system calculations.

The cooling air enters the bearing cavity through hollow first-stage power turbine nozzles. This is the most convenient means of providing entry, and cooling of the nozzles is not necessary or intended. An estimated design of the power turbine nozzles showed that about 30 nozzles would be used, with a total cross section of about 8 sq in. A total flow area of only 2 sq in. will result in an air velocity of 150 ft/sec through the nozzles, which is adequate. Double wall inserts could be used, if necessary, to "spoil" heat transfer, to achieve minimum air-temperature rise prior to cooling of the gasifier blades. To account for unavoidable heat absorption enroute, however, a temperature rise of 95°F, exclusive of hot-gas leakage and compression in the wheel, was used in the system design.

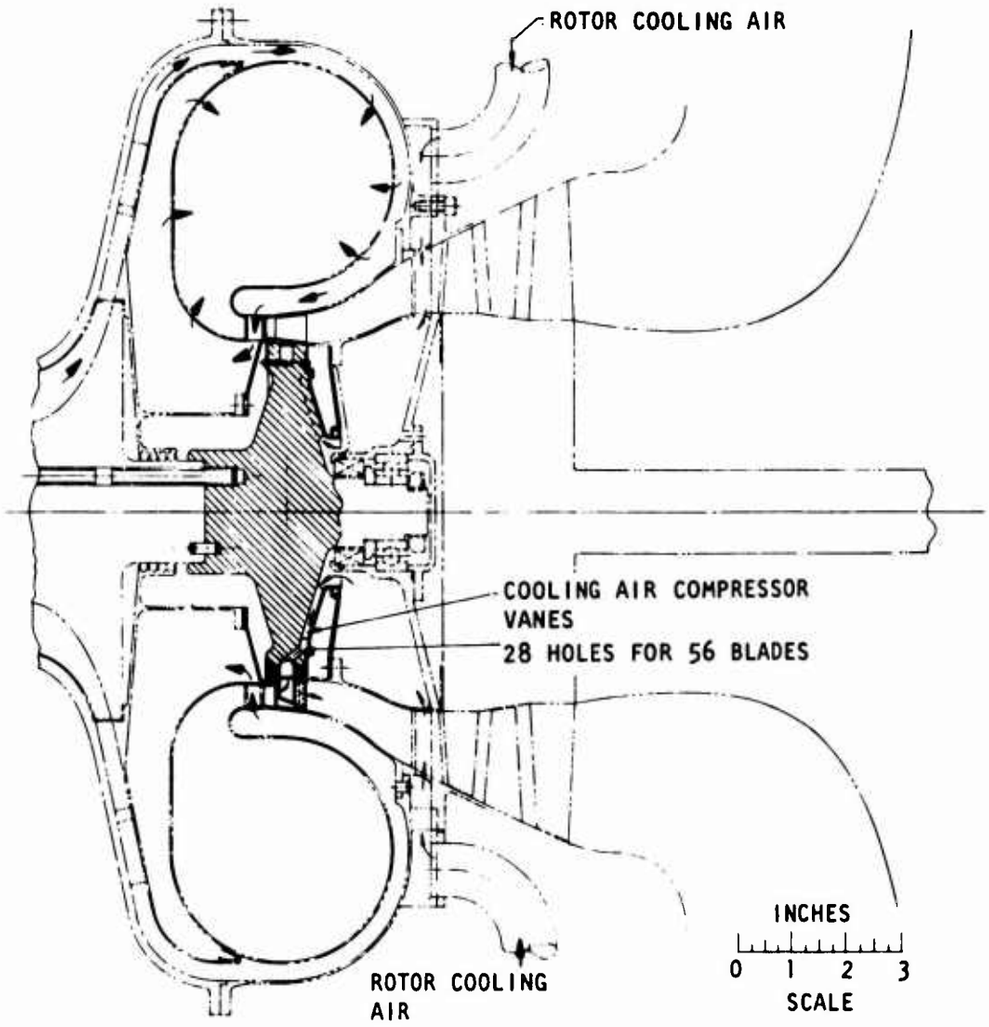

Figure 36. Design Layout of Selected Configuration

The cooling air enters the side-wheel compressor from the bearing cavity. The bearing cavity is sealed from the gasifier turbine exhaust region by a two-step labyrinth, sealing against the OD of the compressor shroud. With a reasonable radial clearance of 0.003 in., the leakage of cooling air at 97 psia to the exhaust at 59.3 psia is 6 pct of the cooling airflow.

The intake annulus area of the side-wheel compressor is sufficient at 0.1-inch vane depth to provide an inlet radial velocity of about 600 ft/sec, with a static intake pressure of 88 psia. The area that would be provided by drilled holes in the hub region would be far less, even with considerable weakening of the disc structure, which would mean extremely high velocities and losses. Furthermore, the tangential velocity of 730 ft/sec would result in oblique entry of the gas into axially drilled holes which probably would result in choking. With a vaned impeller, the correct and efficient incidence can be obtained with a vane angle of about 45 degrees.

The presence of the integrally machined vanes on the wheel will not affect the disc structural design. Although not accomplished under this contract, the shape of the vanes may be efficiently designed, probably with "splitter" vanes toward the outer periphery, to reduce internal friction losses to a minimum. This is essential to the system effectiveness, because a poor efficiency of compression would result in a loss in available pressure and flow, and consequent reduction in velocity and heat transfer effectiveness in the cooled blade passages.

The vanes of the side-wheel compressor are enclosed by a thin (0.030 inch) shroud to prevent the escape of air at the outer periphery. The shroud is attached primarily by welding under a small lip at the rim, but also by spot-welding to the vane edges at intervals. This is shown more clearly in Figure 31. Attachment by welding is considered feasible because the regions of the welds are at the extremities of thin sections, an arrangement which provides inherent thermal isolation from the temperature-sensitive, high-strength disc.

The side-wheel compressor is essentially of a radial type, but with one essential difference: all of the head is produced inside the rotating element by the centrifugal effect. The specific speed of the unit is in a range of low efficiency in conventional compressors with stationary exit diffusers, which is where most of the losses occur (Reference 1). Because the side-wheel compressor does not depend on a stationary exit diffuser, with its high relative gas velocities, to convert the kinetic energy to available pressure, the unit is capable of relatively high compression efficiency. A preliminary estimate of 80 pct has been used for the cooling system calculation. This results in an available cooling air pressure at the blade insert of 180 psia at a temperature of 860°F.

Because of the centrifugal compression effect in the turbine wheel, a temperature rise of about 240°F will occur regardless of the efficiency of compression or the source of air intake. If the main compressor discharge (235 psia, 830°F) were taken as the source, the initial temperature of the cooling air would be 1070°F, which was believed to be too high for effective

blade cooling. Using the discharge of the 2.8:1 axial compressor as a source was not expected to provide enough pressure for effective cooling. The initial pressure within the blade must be sufficiently above the 59.3 psia turbine exhaust pressure to provide adequate velocity in the cooled blade passages. A source of cooling air at 108 psia and 525°F was chosen. This must be taken off the main radial compressor rotor somewhere between inlet and discharge. A special bleed annulus with separate diffusion can be provided to accomplish the bleed effectively.

It should be noted that the selection of the source of cooling air is a suboptimization which was not completely explored. It is possible that a different selection may result in a cooling power penalty lower than the 11 pct which results from the 108 psia, 525°F source.

RESULTS OF THE DETAILED ANALYSIS

FINAL PERFORMANCE ESTIMATE

No changes were necessary in the selected configuration, as a result of the detailed analysis, with regard to structure and internal performance. The rotor was found to be adequate structurally as designed with a blade material of IN-100 and a disc material of INCO 718. The technique of providing cooling air through the wheel with external vanes along the sides caused no change in the original disc structural design. The changes which made a final performance estimate desirable were concerned only with evaluating the selected technique of air cooling with regard to net engine performance and slightly altered design conditions.

The compression of the cooling air in the wheel was not charged as a penalty because the turbine wheel and radial compressor tip diameters are nearly equal. Bleeding of compressor air from within the radial stage reduces the flow through that element and transfers it to the wheel, but the total work of compression is very nearly the same. The cooling air does bypass the gasifier turbine nozzles, however, and in so doing requires a larger pressure drop across the gasifier turbine so as to accomplish the same work of compression with a reduced flow. The heat removed from the gasifier turbine blades also must be subtracted from the available energy through the gasifier turbine, thus requiring an even larger pressure drop. A small part of the energy "borrowed" from the turbine in this latter manner is "restored" through the mixing of the heated cooling air upstream of the power turbine, but an entropy change and a finite loss must be the net result. A further, though relatively minor, loss from the power turbine is incurred by the reduction of the inlet temperature by the mixing of the lower-temperature cooling air.

The combined effect of these penalties appears as a reduced pressure drop and available energy across the power turbine. The cooling system therefore appreciably affects the compressor matching and engine performance. Some differences in the ranges of optimum performance in terms of cycle pressure ratio, inlet temperature, and gasifier speed would undoubtedly result from a repeat of the surveys with cooling. The assumption in this study has been that these are not appreciable, but a more careful design should be done at a later date, with a complete optimization including the cooling penalties.

The approach used in making the final estimate of design and performance with cooling was to assume that the gasifier turbine flow is reduced by the amount of cooling air and that the turbine efficiency is reduced in proportion to the quantity of heat removed. A larger pressure drop will therefore be required. The effect of the regenerative nozzle cooling was included by arbitrarily increasing the burner pressure loss from 2 to 6 pct. A revised matched engine calculation was made on this basis.

It should be mentioned that the increase in gasifier turbine trailing-edge thickness from 0.020 to 0.040 inch for the cooled blade design was not

chargeable as a loss because the discharge of cooling air at about 1700 ft/sec through the slotted trailing edge will actually reduce the wake effect. However, the resulting improvement was not taken into account either. The assumption of 0.020 inch was maintained as a conservative measure, perhaps in compensation for the small entrainment loss at the rotor inlet from the leakage of about 1/2 pct of the compressor discharge air into the turbine nozzle exit chamber.

DESIGN DATA AND PART-LOAD PERFORMANCE

The design data from the final performance estimate are given in Table II.

Part-load performance of the gasifier turbine down to the 40-pct power level was calculated using the fixed hardware corresponding to the design data in Table II. This calculation was made in an engine context, using the compressor performance map shown in Figure 37. The corresponding turbine performance map and operating line are shown in Figure 38. The part-load performance includes the effect of off-design incidence to the turbine blades and cooling of the turbine. The amount of cooling air was assumed to be proportional to the turbine speed. The heat extracted was assumed to be proportional to the product of the 0.8 power of cooling airflow and the turbine inlet temperature. The back pressure was assumed to be controlled by the inlet to the multistage power turbine exhausting to ambient pressure. Off-design back pressures were calculated by the law of the ellipse (Reference 5), based on the design point power turbine inlet.

The efficiency contours shown in Figure 38 reflect the fact that the optimum rotational speed and pressure ratio for the gasifier system were higher than the optimum for the turbine alone. This may also be seen in the curves of gasifier turbine performance in Figure 18. The efficiency of the turbine is rather flat in the region of operation down to 40-pct power level, varying only one point over the range. The variation of compressor efficiency is much sharper, so the design point is closer to the peak performance region of the compressor. The fact that higher part-load turbine efficiencies are achieved at low pressure ratios and speeds also indicates that the effect of off-design incidence had a very minor effect. The maximum incidence angle along the operating line was 8 degrees.

TABLE II

FINAL DESIGN DATA

CYCLE CONDITIONS	
Cycle Pressure Ratio	16.0
Turbine Inlet Temperature, °F	2300.0
Gasifier Speed, rpm	63,300.0
Compressor Airflow, lb/sec	5
Compressor Efficiency, pct	81
Cooling Airflow, lb/sec	0.31
GASIFIER TURBINE DESIGN	
Inlet Total Pressure, psia	221.0
Exit Static Pressure, psia	50.6
Pressure Ratio	4.37
Reaction	0.33
Pitch-Line Velocity Ratio (U_p/C_o)	0.512
Nozzle Exit Mach Number	1.241
Rotor Inlet Relative Mach Number	0.576
Rotor Exit Relative Mach Number	1.07
Specific Speed	59.2
Specific Diameter	1.428
Effective Gas Recovery Temperature, °F	1877
Blade-Root Temperature, °F	1370
Turbine Tip Speed, ft/sec	1900
Total-to-Total Efficiency, pct	90.6
Total-to-Static Efficiency, pct	83.4
Gasifier Turbine Shaft Power, hp	1307.4
NET ENGINE PERFORMANCE (WITH COOLING)	
Specific Horsepower, hp-sec/lb	203.6
Net Engine Power, hp	1018.0
Thermal Efficiency, pct	0.294
Specific Fuel Consumption, lb/hp-hr	0.470
Cooling Power Penalty, pct	11.1

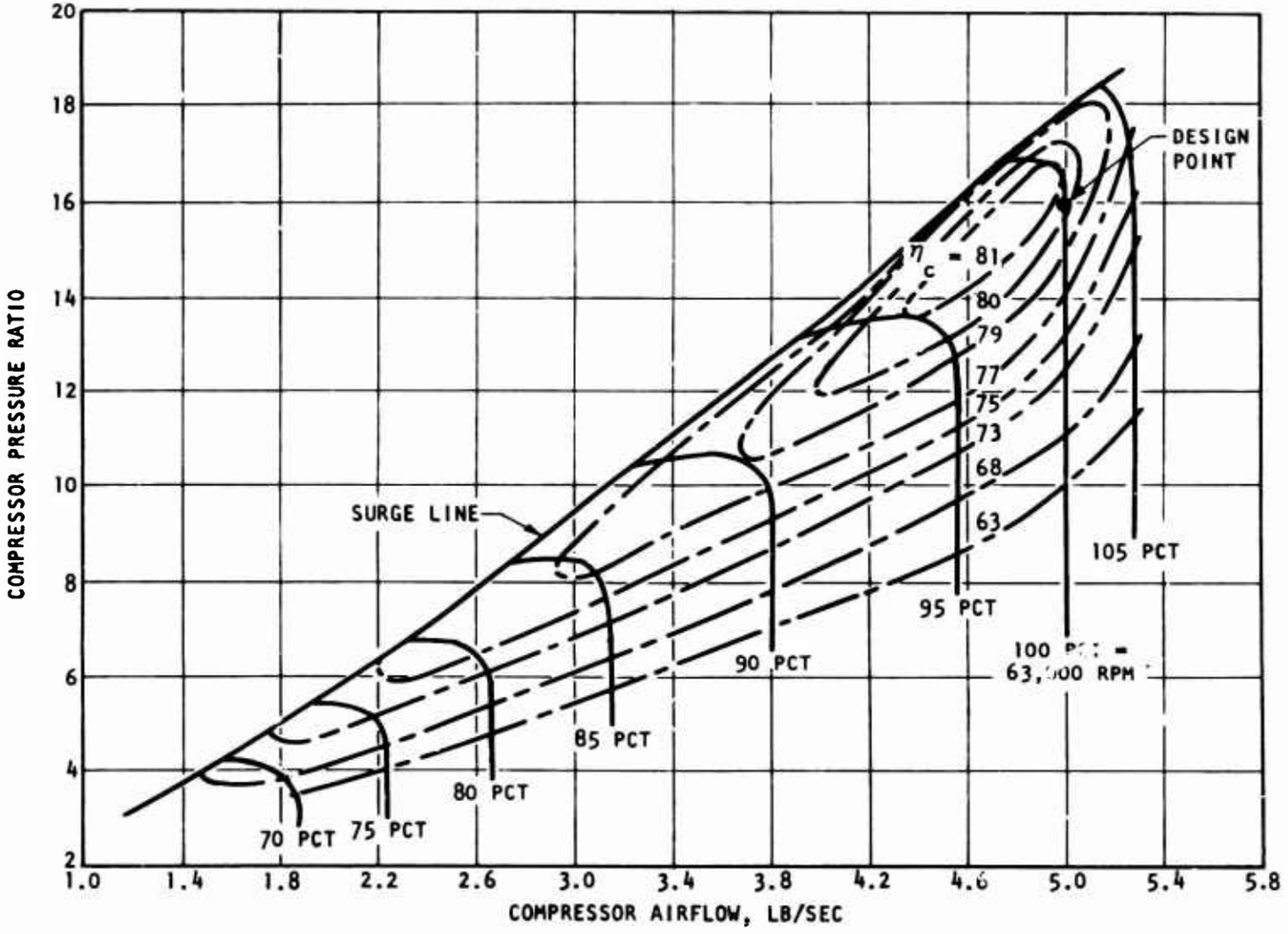

Figure 37. Compressor Map for Part-Load Performance

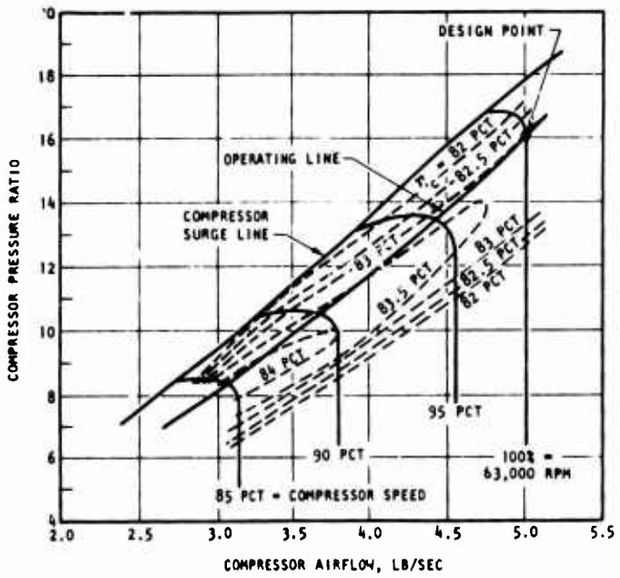

a. Efficiency

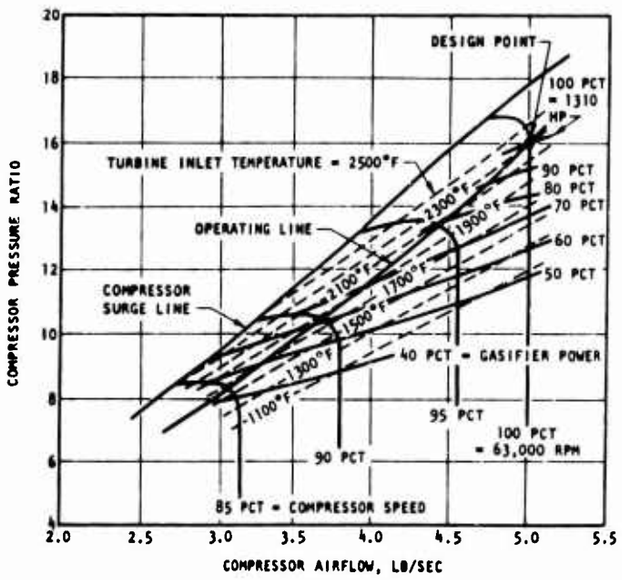

b. Temperature and Power

Figure 38. Part-Load Turbine Performance Map

CONCLUSIONS

The major conclusion of this study is that a single-stage, axial-flow gasifier turbine for the intended application is very competitive in performance, with no Mach number penalties, within safe allowable stress limits of materials now available, and is practical to build using current advanced fabrication techniques. It should result in significant improvements in weight, volume, simplicity, and in a reduction in cost over multistaged components. There is a broad efficient design range over the full intervals of inlet temperatures and cycle pressure ratios investigated, but effective cooling is required and is paramount in importance above 1700°F inlet temperature.

Turbines in the regions of best overall engine performance were found to be in the high subsonic to transonic regime, well below levels where losses resulting from local supersonic effects are incurred. The transonic regime is approached only when severe allowable stress limits exist because of high blade temperatures stemming from lack of effective cooling. The impaired performance in these cases is caused primarily not by the local supersonic effects, but by the restriction of the blade height and resulting rotor annulus caused by the low allowable stress. The reduced blade height causes the efficiency to drop quickly to unacceptable levels because of increased exhaust and internal friction losses. Because of the restriction in annulus area, the Mach numbers become higher for these designs and approach the high transonic regimes. Further increase in temperature causes choking of the rotor exit annulus at design speeds below the optimum, which further impairs performance.

In view of the sharp sensitivity of gasifier turbine and engine performance to increased blade temperature above 1200°F, it is significant that the optimum rotor relative inlet Mach numbers are always subsonic, eliminating the need for thin, sharp-leading-edge, supersonic blade designs. This greatly facilitates the development of effective blade cooling techniques.

The precise determination of the optimum blade temperature and inlet temperature is a function of the effectiveness of the cooling technique used, and involves maximizing the net engine output, including the effect of the cooling power penalty on engine component matching, design, and performance. Although inclusion of the complete effects of cooling in the optimization was beyond the scope of the program, the generalized study included the effect of a reasonable heat load on blade temperature. With practical tapered blades, designed for proper cooling and cast from IN-100, which is one of the better high-temperature materials currently available, the performance of turbines in the 1350°to 1450°F blade-root-temperature range is acceptably high (84-pct gasifier turbine total-to-static efficiency) in spite of moderately stress-limited blade heights. Any significant increase in blade temperature above this level will result in severely reduced performance because of material strength limitations.

The generalized analysis showed the comparison given in Table III for cooled machines at two levels of cooling (in terms of the pct of net engine power consumed by cooling) against an uncooled machine at the highest practical

inlet temperature. It will be noted that at a blade-root temperature of 1670°F, the gasifier turbine efficiency is reduced to 69 pct by the low blade height resulting from reduced allowable stress. This illustrates and reflects the steep "dive" in strength which is typical of all available materials in this temperature range. These results are based on strict adherence to minimum margins of safety established for the intended equipment mission and duration at the beginning of the study.

TABLE III

GENERALIZED COMPARISON OF COOLED AND UNCOOLED ENGINE PERFORMANCE (COMPRESSOR PRESSURE RATIO 16:1)

Parameter	Cooling Power Penalty, Percent of Net Engine Power		
	0 (uncooled)	8	4.6
Inlet Temperature, °F	1700	2300	2300
Blade-Root Temperature, °F	1370	1370	1670
Gasifier Turbine Efficiency, Total-to-Static	0.846	0.841	0.690
Relative Net Specific Power	1.0	1.7	1.08
Relative Net Specific Fuel Consumption	1.0	1.0	1.3

Table III shows that the potential advantage of high inlet temperatures is a substantial increase in specific power without increase in specific fuel consumption, but it is dependent on the ability to effectively cool the gasifier turbine to reasonably low blade-root temperatures without excessive power penalty. If a blade-root temperature between 1350° and 1450°F can be achieved with 8 pct cooling power penalty, a 70-pct increase in specific power at 2300°F, can be realized over an uncooled machine.

The specific air-cooling technique selected for the detailed design resulted in a blade-root temperature slightly below 1450°F, but did not quite meet the target power penalty of 8 percent. This technique is one of the more feasible, but less advanced, of the cooling techniques now under development. The performance of the final design, with cooling effects included in the net power and fuel consumption, is given in Table IV. The system has a cooling power penalty of 11 pct and provides an increase in net specific power at 2300°F of 62 pct over that of the maximum-temperature uncooled engine, with an increase in specific fuel consumption of 1 pct.

TABLE IV

FINAL PERFORMANCE SUMMARY

Gasifier Turbine Total-to-Static Efficiency, pct	83.4
Gasifier Turbine Total-to-Total Efficiency, pct	90.6
Net Engine Specific Power, hp-sec/lb	203.6
Net Specific Fuel Consumption, lb/hp-hr	0.470
Cooling Power Penalty, pct	11.1

The attainment of a high blade speed is important in a single-stage, high-pressure-ratio application in order to utilize the high kinetic energy effectively. Traditionally, axial turbine manufacturers have avoided blade tip speeds above 1600 ft/sec because of the high stresses involved with the blade heights they were using. This study showed that in the range of the investigation, the internal performance tradeoff between blade height and tip speed was weighted heavily in favor of the tip speed In all cases, it was found that running the tip speed at the full limit imposed by the disc stress, in spite of limitations in blade height and annulus area, resulted in significantly improved performance The advantage of attaining a tip speed of 1900 ft/sec by shortening the blades slightly, was demonstrated, and feasibility was verified by the detailed stress analysis.

RECOMMENDATIONS

The following recommendations are presented in order of relative importance.

VERIFICATION OF PERFORMANCE

The turbine efficiencies predicted in this study are considerably higher than some current tests of high-work, low-aspect-ratio turbines in the same specific speed range. These high efficiencies are believed to be attainable and stem from the improved optimization of the design by the technique described in this report. Although it has been shown (Figure 4) that the prediction technique agrees well with test data above and below the specific speed range, there is need for more valid tests in the same range to verify that the improved performance can be achieved. Such tests should be carefully planned to eliminate extraneous influences such as initial boundary layer effect and low Reynolds number caused by testing at reduced exhaust pressures. It is recommended that a series of tests, beginning with cascade investigations to verify internal loss relations at low aspect ratio and culminating in a rotating test to include centrifugal effects, be undertaken.

ENGINE SYSTEM OPTIMIZATION

Because of the considerable influence of cooling technique effectiveness on the gasifier turbine matching and design and on the net engine performance, it is recommended that these studies be continued toward optimization of the single-stage gasifier turbine in conjunction with a complete engine system. Various cooling techniques should be compared by detailed analysis similar to the one in this report, as to their optimum effectiveness levels and relative merits in the engine system.

Furthermore, an analysis of the entire system would permit inclusion of the heat transfer aspect in the optimization of the gasifier turbine geometry, in addition to the stress and internal performance aspects which have been included so far. Results in this report clearly indicate that changes in blade heat transfer area, such as by reducing blade height or by decreasing the number of blades, have a predominant influence on blade-root temperature. Assessment of the tradeoffs of these measures with stress and efficiency can be made only by including the effect of cooling on overall engine performance.

EVALUATION OF AIR-COOLING TECHNIQUE

Further evaluation of the technique of air-cooling shown in this report is recommended, particularly in regard to design of the "side-wheel compressor". It is believed that this system should be competitive with more complex advanced techniques with fewer inherent development problems.

BIBLIOGRAPHY

1 Balje, O. E., "A Study of Design Criteria and Matching of Turbomachines," Transactions of the ASME, Journal of Engineering for Power, January 1962.

2 Bauermeister, K. J., "About the Influence of the Blade Load on the on the Secondary Flow in Straight Turbine and Compressor Cascades," (in German), VDI-Forschungsheft 496, Diisseldorf, 1963, p. 27.

3 Barningham, R. C., Third Semiannual Report on Component Propulsion Program for Future High Performance Aircraft, (Unclassified Title), Volume XI, P&W Aircraft for ASD-AFSC, Wright-Patterson AFB, Ohio, February 1967, (CONFIDENTIAL).

4 Bolte, W., "On the Calculation and Optimization of the Efficiency of Axial Flow Machines," (in German), VDI-Forschungsheft 501, Essen, 1964, p. 18.

5 Csanady, G. T., Theory of Turbomachines, McGraw-Hill, New York, 1964, p. 18.

6 Eckert, E. R. G., and Drake, R. M., Heat and Mass Transfer, Second Edition, McGraw-Hill, New York, 1959.

7 Horlock, J. H., Axial Flow Turbines, Butterworths, London, 1966, p. 86.

8 Huppert, M. C., and MacGregor, C., "Comparison Between Predicted and Observed Performance of a Gas Turbine Stator Blade Designed for Free Vortex Flow," NACA Tech. Note No. 1810, 1949

9 International Nickel Co., Inc., High Temperature High Strength Nickel Base Alloys, Revised Edition, 1964.

10 McCormick, H. L. and Reed, J. H., "Evaluation of the Cast Internally Cooled Airfoil," SAE Paper 280B, January 1961.

11 Moffitt, T. P., "Design and Experimental Investigation of a Single Stage Turbine with a Rotor Entering Relative Mach Number of 2," NACA Research Memorandum RM E58F20a, September 1958

12 Nusbaum, J., et al, "Experimental Investigation of a High Subsonic Mach Number Turbine Having a 40-Blade Rotor With Zero Suction Surface Diffusion," NACA Research Memorandum RM E57J22, January 1958.

13 Rocketdyne Report R-6805, Turbine Performance Prediction: Optimization Using Fluid Dynamic Criteria, December 1966.

14 Schlichting, H., Boundary Layer Theory, Fourth Edition, McGraw-Hill, New York, 1960, p. 80.

15 Stewart, W. L., et al, "A Study of Boundary Layer Characteristics of Turbomachine Blade Rows and Their Relation to Over-All Loss," Transactions ASME, Series D, Vol. 82, No. 3, September 1960, p. 588-592.

16 Traupel, W., Thermische Turbomaschinen, Volume I, Second Edition, Springer Verlag, Berlin, 1966, p. 364.

17 Van Driest, E. R., Recent Studies in Boundary Layer Transition, North American Aviation, Inc., SID Report 64-546, AFOSR 64-0589, November 1963.

18 Whitney, W. J., et al, "Investigation of a Transonic Turbine Designed for Zero Diffusion of Suction-Surface Velocity," NACA Research Memorandum RM E54F23, August 1954.

19 Wolf, H., Die Randverluste in Geraden Schaufelgittern, Wissenschaftliche Zeitschrift der Technischen Hochschule Dresden, 10, Heft 2, 1961.

20 Wood, C. F., Recent Developments in Direct Search Techniques, Westinghouse Research Laboratories Research Report 62-159-522-R1, July 1962.

21 Zweifel, O., "The Spacing of Turbomachine Blading, Especially With Large Angular Deflection," The Brown Boveri Review, December 1945, p. 436-444.

UNCLASSIFIED

Security Classification

DOCUMENT CONTROL DATA - R & D

(Security classification of title, body of abstract and indexing annotation must be entered when the overall report is classified)

1 ORIGINATING ACTIVITY (Corporate author) Rocketdyne, a Division of North American Rockwell Corporation Canoga Park, California	2a. REPORT SECURITY CLASSIFICATION UNCLASSIFIED 2b. GROUP

3 REPORT TITLE

A STUDY OF HIGH-MACH-NUMBER, HIGH-TEMPERATURE APPLICATION OF A SMALL, SINGLE-STAGE, AXIAL-FLOW GAS TURBINE

4 DESCRIPTIVE NOTES (Type of report and inclusive dates)

Final Report (6 February 1967 to 5 November 1967)

5 AUTHOR(S) (First name, middle initial, last name)

David H. Cooke

6 REPORT DATE June 1968	7a. TOTAL NO OF PAGES 90	7b. NO OF REFS 21
8a CONTRACT OR GRANT NO DAAJ02-67-C-0011 b. PROJECT NO c. Task 1M125901A01409 d	9a. ORIGINATOR'S REPORT NUMBER(S) USAAVLABS Technical Report 68-34 9b. OTHER REPORT NO(S) (Any other numbers that may be assigned this report) R-7261	

10 DISTRIBUTION STATEMENT

This document has been approved for public release and sale; its distribution is unlimited.

11 SUPPLEMENTARY NOTES	12 SPONSORING MILITARY ACTIVITY U.S. Army Aviation Materiel Laboratories Fort Eustis, Virginia

13 ABSTRACT

This report presents the results of a study to determine the merit and feasibility of using a single-stage axial turbine as a compressor drive (gasifier) turbine in a small, high-temperature, high-pressure-ratio, turboshaft/free-shaft engine. Turbine inlet temperatures up to 2300°F, with cooling, compression ratios from 16:1 to 20:1 and shaft speeds from 50,000 to 70,000 rpm were investigated. Results of a generalized analysis showed that with cooling there is a broad design range with acceptable and competitive engine performance, within allowable stress limitations, over the full intervals of inlet temperature and pressure ratios investigated. Rotor inlet Mach numbers were found to be subsonic over the entire range, which eliminates the need for thin, sharp-leading-edge, supersonic blade designs, thus simplifying rotor blade cooling problems at high temperatures. The major conclusions of the study are that single-stage, axial-flow gasifier turbines for the intended application are competitive in performance, have no Mach number penalties, are practical to build, and are within the reach of current advanced technology.

DD FORM 1 NOV 65 1473

UNCLASSIFIED

Security Classification

UNCLASSIFIED
Security Classification

14. KEY WORDS	LINK A		LINK B		LINK C	
	ROLE	WT	ROLE	WT	ROLE	WT
Axial Flow Gas Turbine Stage						
Aerodynamic Loading						
Stress Relations						
Design Criteria						
Cooling Effects						
Turbine Performance						
Sonic Conditions						
Mach Number Effects						

UNCLASSIFIED
Security Classification

669 1-68